**Accumulation of amyloid-β in the brain of mouse models of Alzheimer's disease is modified by altered gene expression in the presence of human apoE isoforms during aging**

Keiko Honda[1,2], Yuhki Saito[3], Haruka Saito[1,2], Megumi Toyoda[1], Ruriko Abe[2], Takashi Saito[4], Takaomi C. Saido[5], Makoto Michikawa[6], Hidenori Taru[1,2], Yuriko Sobu[1,2], Saori Hata[1,2,7], Tadashi Nakaya[1,8], *Toshiharu Suzuki[1,2]

[1]Laboratory of Neuroscience, Graduate School of Pharmaceutical Sciences, Hokkaido University, Sapporo 060-0812, Japan.

[2]Advanced Prevention and Research Laboratory for Dementia, Graduate School of Pharmaceutical Sciences, Hokkaido University, Sapporo 060-0812, Japan.

[3]Laboratory of Molecular Neuro-Oncology, The Rockefeller University, 1230 York Avenue, NY 10065, USA.

[4]Department of Neurocognitive Science, Institute of Brain Science, Nagoya City University Graduate School of Medical Sciences, Nagoya 467-8601, Japan.

[5]Laboratory for Proteolytic Neuroscience, RIKEN Center for Brain Science Institute, Wako 351-0198, Japan.

[6]Department of Biochemistry, Nagoya City University Graduate School of Medical Sciences, Nagoya 467-8601, Japan.

[7]Biomedical Research Institute, National Institute of Advanced Industrial Science and Technology (AIST), Tsukuba 305-8566, Japan.

[8]School of Pharmacy of Fukuoka, International University of Health and Welfare, Fukuoka 831-8501, Japan.

*Correspondence to Toshiharu Suzuki (tsuzuki@pharm.hokudai.ac.jp), Advanced Prevention and Research Laboratory for Dementia, Graduate School of Pharmaceutical Sciences, Hokkaido University, Kita12-Nishi6, Kita-ku, Sapporo 060-0812, Japan.

**Abbreviations:** Aβ, amyloid-β; AD, Alzheimer's disease; apoE, apolipoprotein E; APP, amyloid β-protein precursor; CVF, cerebroventricular fluid; ELISA, enzyme-linked immune sorbent assay; KI, knock-in; PIC, protease inhibitor cocktail.

***Abstract***

Apolipoprotein E4 (apoE4) is a risk factor for Alzheimer's disease (AD). Here, we investigated brain amyloid-β (Aβ) accumulation throughout the aging process in an amyloid precursor protein (APP) knock-in (KI) mouse model of AD that expresses human $APP^{NL\text{-}G\text{-}F}$ with or without human apoE4 or apoE3. Brain Aβ42 levels were significantly lower in 9-month-old mice that express human isoforms of apoE than in age-matched APP-KI control mice. Linear accumulation of Aβ42 began in 5-month-old apoE4 mice, and a strong increase in Aβ42 levels was observed in 21-month-old apoE3 mice. Aβ42 levels in cerebroventricular fluid were higher in apoE3 than in apoE4 mice at 6–7 months of age, suggesting that apoE3 is more efficient at clearing Aβ42 than apoE4 at these ages. However, apoE3 protein levels were lower than apoE4 protein levels in the brains of 21-month-old apoE3 and apoE4 mice, respectively, which may explain the rapid increase in brain Aβ42 burden in apoE3 mice. We identified genes that were downregulated in a human apoE-dependent (apoE4>apoE3*)* and age-dependent (apoE3=apoE4) manner, which may regulate brain Aβ burden and/or AD progression. Analysis of gene expression in AD mouse models helps identify molecular mechanisms of pleiotropy by the human *APOE* gene during aging.

***Keywords***

***Alzheimer's disease, amyloid-β, apolipoprotein E, gene expression, brain aging***

## 1. Introduction

Alzheimer's disease (AD) is the most common neurodegenerative disease in the aged population and is characterized by the progressive loss of memory and cognitive functions. Approximately 50 million patients live with dementia worldwide, and AD accounts for 60–80% of these cases (**2021 Alzheimer's disease facts and figures**). The vast majority of patients with AD have the sporadic or late-onset form of the disease, whereas several percent of patients with AD have familial AD and carry pathogenic mutation(s) in the causative genes *App*, *PSEN1*, and *PSEN2.* The *App* gene encodes amyloid-β protein precursor (APP) from which neurotoxic Aβ peptides are generated. *PSENs* encode presenilin 1 and 2 (PS1 and PS2), which are the catalytic component of γ-secretase complex **(Selkoe 2011**). Pathogenic mutations in the *App* gene increase the amount of Aβ or the production of neurotoxic Aβ42 peptides (**Mullan et al., 1992; Di Fede et al., 2009; Zhou et al., 2011**). A protective mutation in the *App* gene decreases Aβ generation by inducing the amyloidolytic cleavage of APP at β'-site by β-site APP-cleaving enzyme 1 (BACE1), which is the primary enzyme responsible for Aβ generation (**Jonsson et al., 2012; Kimura et al., 2016**). Following the amyloidogenic processing of APP at β-site by BACE1, γ-secretase complex cleaves the membrane-tethered APP carboxyterminal fragment (APP CTFβ or C99) to produce Aβ species (**Cole & Vassar, 2008; Thinakaran & Koo, 2008**). Pathogenic mutations in *PSEN* genes increase the generation of Aβ42 peptide species. Thus, the generation and production of neurotoxic Aβ oligomers are strongly believed to be the primary triggers of neurodegeneration in AD (**Benilova et al., 2012**).

In contrast to familial AD, the main cause(s) of sporadic AD is controversial. Although the major risk factor is older age, the greatest genetic risk factor for late-onset AD is the ε4 allele of *APOE* (**Corder et al., 1993**). In individuals carrying one of three alleles, ε2 (apoE2), ε3 (apoE3), or ε4 (apoE4), the apoE4 genotype (ε3/ε4, or ε4/ε4) increases the risk of developing early-onset AD compared with non-apoE4 carriers (**Raber et al., 2004**). ApoE is reported to serve a variety of functions in AD pathophysiology in addition to its major role in lipid metabolism (**Martens et al., 2022**). For example, apoE4 has a weaker ability than apoE2 and apoE3 for clearing Aβ in the brain (**Castellano et al., 2011; Hashimoto et al., 2012**). ApoE is thought to play an important role in organelle homeostasis such as ER stress and mitochondrial dysfunction which induce and/or progress neurodegeneration (**Ridge & Kauwe 2018; Swerdlow et al., 2014**). In the central nervous system (CNS), apoE is expressed in non-neuronal cells and mainly in astrocytes, and neurons express apoE in response to injury (**Xu et al., 2006**), suggesting a progressive or repressive function of apoE in neurodegeneration.

Recent studies report that apoE4 drives lipid metabolic dysregulation in astrocytes and microglia, and induces matrisome dysregulation that increases glial activation (**TCW et. al., 2022**). However, the pleiotropic contribution of apoE isoforms in the pathogenesis of and/or the

progression of AD in aging remains controversial. In this study, by focusing on changes in Aβ levels and gene expression in the aging brain, we investigated whether apoE4 and apoE3 function similarly or differently during the continuous progression of AD with age. Using mouse models of AD, we show here the impact of different apoE isoforms on Aβ accumulation at different ages in the brain. Furthermore, we also discuss how changes in the expression of genes that possibly regulate brain Aβ burden may depend on human apoE rather than on specific apoE isoforms in the aged brain.

## 2. Materials and Methods

### 2.1 Generation of double gene knock-in (KI) mice

*App*$^{NL\text{-}G\text{-}F/NL\text{-}G\text{-}F}$ (C57BL/6-App<tm3(NL-G-F)Tcs, RRID:IMSR_RBRC06344) (**Saito et al, 2014**), ApoE3-KI (B6;129-Apoe<tm3(APOE3)sfu>/sfuRbrc, RRID:IMSR_RBRC03390), and ApoE4-KI (B6;129-Apoe<tm3(APOE4)sfu>/sfuRbrc RRID:IMSR_RBRC03418) mice (**Hamanaka et al., 2000; Mori et al., 2003**) were housed in specific pathogen-free (SPF) conditions with a microenvironment ventilation system (Allentown Inc., Allentown, NJ, USA) under a 12 h light-dark cycle and had free access to food and water. Three to five male or female siblings were housed in each cage with a floor space of 535 $cm^2$ that had micro barrier tops. All animal studies were conducted in compliance with the ARRIVE guidelines and all experimental protocols were approved by the Animal Care and Use committees of Hokkaido University and RIKEN Center for Brain Science Institute. Human apoE3 and apoE4 gene KI mice were backcrossed with C57BL6/J mice for 12–13 generations, and the APP-KI/apoE3 and APP-KI/apoE4 mice were generated by mating with *App*$^{NL\text{-}G\text{-}F/NL\text{-}G\text{-}F}$ (APP-KI) mice. Homologous double KI mice were used for experiments. To exclude possible differences because of gender, we used only female mice for all our analyses.

### 2.2 Extraction and quantification of brain Aβ

Brain lysates for the Aβ assay were prepared as described (**Kondo et al., 2010**) with a few modifications. Briefly, the cerebral cortex and hippocampus from the left hemisphere of the brain were dissected and then homogenized on ice for 30 strokes with a Dounce homogenizer in a 4-fold volume of TBS (20 mM Tris-HCl, pH 7.4 containing 137 mM NaCl) and protease inhibitor cocktail (PIC) (5 μg/mL chymostatin, 5 μg/mL leupeptin, and 5 μg/mL pepstatin). The lysate was subject to centrifugation (200,000 x g for 20 min at 4ºC) with TLA 100.4 rotor (Beckman Coulter Life Science, Brea CA, USA). The resultant precipitate was further homogenized in a 9-fold volume of TBS with a Dounce homogenizer for 30 strokes, and was then centrifuged at 100,000 × g for 20 min at 4 ºC with TLA 55 rotor (Beckman Coulter Life Science). The pellet was dissolved in an equal volume of 6 M guanidine-HCl solution in 50 mM

Tris-HCl (pH 7.6) with sonication (1 second with a 1 second interval of 17 cycles, with SONICSTAR85, WAKENYAKU, Co., Kyoto Japan) and left to stand for 1 h at room temperature. The sample was then centrifuged at 130,000 × g for 20 min, and the supernatant was used for Aβ40 and Aβ42 assays. Human Aβ40 and Aβ42 were quantified by sandwich ELISA (sELISA) as described previously (**Tomita et al., 1998**), with the exception that the 82E1 antibody (Immuno Biological Laboratories, Fujioka, Japan, Cat 10323) rather than the 2D1 antibody was used (**Mizumaru et al., 2009**).

**2.3 Preparation of brain lysates and immunoblotting**

The cerebral cortex and hippocampus from the right hemisphere of the brain were homogenized on ice for 30 strokes with a Dounce homogenizer in a 10-fold volume of buffer H (20 mM HEPES, pH 7.4, containing 150 mM NaCl, 5 mM EDTA, 10% (v/v) glycerol, and PIC). An aliquot (200 μL) of the lysate was diluted with an equal amount of 2× RIPA buffer (100 mM Tris-HCl (pH 7.6) containing 300 mM NaCl, 2% (v/v) Nonidet P40, 1% (w/v), sodium deoxycholate, 0.2% (w/v) SDS and 2× PIC) and sonicated (1 second with a 1 second interval, 10 cycles). The detergent-solubilized sample was centrifuged at 10,000 × g for 1 min at 4 ºC and the supernatant was used for immunoblotting as total brain lysate. Protein amounts were quantified with the BCA Protein Assay Kit (Cat T9300A, TAKARA, Kyoto, Japan). Indicated amounts of protein lysates were subjected to Tris-glycine SDS polyacrylamide gel electrophoresis (**LaemmlI, 1970**) and separated proteins were transferred onto a nitrocellulose membrane (Cat# P/N66485, Paul Corp., Pensacola, FL, USA) for immunoblotting. Membranes were blocked in 5% (w/v) non-fat dry milk (Morinaga Milk Industry, Tokyo, Japan) in TBS-T (20 mM Tris-HCl [pH 7.6], 137 mM NaCl, 0.05% (v/v) Tween 20 (Cat sc-29113, Nacalai Tesque, Kyoto, Japan)), probed with the indicated antibodies diluted in TBS-T. The membrane was washed with TBS-T, and immunoreactive proteins were detected using Clarity Western ECL substrate (Cat 1705061, Bio-Rad, Hercules, CA, USA) and quantitated on a LAS-4000 imaging system (Fujifilm, Tokyo, Japan). Anti-human apoE (A299) antibody (1:1000 dilution; Cat 18171, IBL), anti-APP antibody 369 (1:5000 dilution) (**Oishi et al 1997**), anti-α-tubulin antibody (1:10,000 dilution, 10G10 Cat 013-25033, Fujifilm Waco Pure Chemicals), anti-mouse IgG HRP-Linked F（ab’）2 Fragment sheep (1:10,000 dilution Cat NA9310, Cytiva, Mariborough, MA, USA), and anti-rabbit IgG HRP-Linked F（ab’）2 Fragment donkey (1:10,000 dilution Cat NA9340, Cytiva) were used.

**2.4 Collection of cerebrospinal and cerebroventricular fluids in mice models of AD.**

Mice were injected intraperitoneally with a mixture of anesthetics (0.3 mg/kg weight medetomidine hydrochloride, Cat 135-17473 FujiFilm Wako; 4 mg/kg weight midazolam, Cat

135-13791 FujiFilm Wako; 5 mg/kg weight butorphanol tartrate, Cat 021-19001 Fujifilm Wako). Cerebrospinal fluid (CSF) was collected from the cisterna magna as described previously (**Liu & Duff, 2008**). Cerebroventricular fluid (CVF) was collected with a micro syringe via a stereotaxic micromanipulator (SMM-100, Narishige, Tokyo Japan) (bregma 1.1 mm, 0.5 mm lateral to the midline, and 2.5 mm ventral to the skull surface). CSF and CVF were quickly frozen in liquid nitrogen and stored in the deep freezer (-80 ºC) until use. These fluids were diluted in PBS buffer containing 1% (w/v) bovine serum albumin and 0.05% (v/v) Tween-20, and Aβ42 was quantified as described above.

**2.5 RNA-seq analysis**

The cerebral cortex and hippocampus from the right hemisphere of the brain were homogenized, and RNA was extracted with TRIzol reagent (Cat 15596018, Thermo Fisher Scientific, Waltham, MA, USA). RNA samples were submitted to Novogene (Beijing, China) via Nippon Genetics (Tokyo, Japan). After performing quality checks of RNA samples, Novogene prepared strand-specific cDNA libraries and subjected the samples to sequencing using NovaSeq 6000 / PE150 sequencing platform. We obtained 10.1 to 14.9 million reads per sample.

**2.6 Processing of RNA-seq data**

The raw sequencing data were mapped to the mouse genome, mm10, by STAR (version 2.7.3a) with a default setting. Differential gene expression analysis was performed with the package "DESeq2" in R **(Love et al., 2014)**. Low-expressing genes (less than 100 RNA-seq reads per gene, on average) were excluded from the analysis. A difference with an FDR smaller than 0.05 was identified as being significant.

**2.7 Gene ontology enrichment analysis**

Gene ontology (GO) analysis was performed with the DAVID Functional Annotation Clustering Tool (DAVID Bioinformatics Resources: https://david.ncifcrf.gov).

**2.8 Quantitative real-time PCR (qPCR)**

Extracted RNA used in RNA-seq analysis was treated with DNase (ThermoFisher TURBO DNase AM2238) and reverse transcribed with PrimeScript™ 1st strand cDNA Synthesis Kit (Takara: 6110A) for qPCR. qPCR was performed with Brilliant III Ultra-Fast SYBR Green QPCR Master Mix (Agilent Technologies: #600882) on the BIO-RAD Touch Real-Time PCR Detection System under the following conditions: 40 cycles; 95 °C (10 s) and 60°C (20 s). Data

were analyzed with the ΔΔCt method and were normalized to *Actb* mRNA levels. The primer sets used for RT-qPCR are shown in Supplementary Table 2.

## 3. Results

### 3.1 Accumulation of brain Aβ in mouse models of AD with isoforms of human apoE during the aging process

To uncover the influence of human apoE isoforms on brain Aβ accumulation during the aging process, we analyzed three lines of the mouse model of AD; $APP^{NL\text{-}G\text{-}F/NL\text{-}G\text{-}F}$/human apoE4 (apoE4 mouse), $APP^{NL\text{-}G\text{-}F/NL\text{-}G\text{-}F}$/human apoE3 (apoE3 mouse), and $APP^{NL\text{-}G\text{-}F/NL\text{-}G\text{-}F}$/mouse apoE (APP-KI mouse). $APP^{NL\text{-}G\text{-}F/NL\text{-}G\text{-}F}$ mice, which harbor the Iberian mutation (I716F) near the γ-secretase cleavage site and the Swedish mutation (K670N/M671L) near the β-secretase cleavage site (**Saito et al., 2014**), generate mainly humanized Aβ42 rather than Aβ40. We investigated Aβ accumulation in the cerebral cortex and hippocampus in these mouse models. The amount of human Aβ in 3-month-old (young adult stage), 5- and 9-month-old (middle adult stages), 13-month-old (early-aged stage), and 21-month-old (late-aged stage) mice was quantified with a sELISA specific for human Aβ. As expected, Aβ40 accumulation increased with age. The accumulation of Aβ40 clearly began in middle adulthood (9 months old) in APP-KI mice, which express endogenous mouse apoE earlier than mice that express either human apoE3 or apoE4. ApoE3 or apoE4 mice began accumulating Aβ40 after 13 months of age, and by 21 months of age, the quantity of Aβ40 was higher in APP-KI mice than in apoE4 and apoE3 mice during the aging process (**Fig. 1A**). These data were consistent with a previous report that human apoE reduces Aβ deposition in a human APP transgenic mouse model of AD (**Holzman et al., 1999**).

Aβ42 accumulation was observed in 3-month-old APP-KI mice and reached saturation (500–600 pmol/g tissue weight) when these mice were 5 months old. Interestingly, this level of Aβ42 was maintained throughout the aging process even at 21 months of age without a noteworthy increase in Aβ42 accumulation in aged mice (**Fig. 1B, C**). In contrast to APP-KI mice, Aβ42 accumulation in apoE4 mice linearly increased after 5 months of age, whereas apoE3 mice at an age of 13 months maintained lower levels of Aβ42. Remarkably, at 21 months old, this level of Aβ42 increased in apoE3 mice and reached a similar level to that in apoE4 mice (> 800 pmol/g tissue). In summary, apoE4 contributed to the continuous accumulation of Aβ42 with age, whereas apoE3 tended to suppress Aβ42 accumulation in early-aged mice. A greater number of aged (21-month-old) mice, expressing either apoE4 or apoE3, accumulated more Aβ42 than APP-KI mice. These observations suggest that human apoE suppresses the accumulation of brain Aβ by the middle adult stage, but is ineffectual in the brain in late-aged mice. The ineffectiveness of human apoE appears earlier in the lifespan in apoE4 mice but later

in apoE3 mice, which may be the primary reason for the later onset of AD in apoE3 than in apoE4 carriers. Our findings in mouse models may be consistent with those in human studies that showed that individuals harboring the apoE3 allele tended to have onset of AD at an older age than those subjects carrying the apoE4 allele (**Raber et al., 2004; Spinney et al., 2014)**.

The levels of Aβ40 and Aβ42 were both higher in APP-KI mice than in apoE3 and apoE4 mice by 9 months of age. This may indicate a lower ability of mouse apoE than of human apoE isoforms to clear Aβ as suggested by a previous study (**Fagan et al., 2002**). Those authors reported the continuous and higher accumulation of Aβ in mouse expressing mouse apoE than in mouse expressing apoE3 and apoE4 during the aging process from 18 to 24 months of age.

To investigate whether human apoE isoforms have a higher ability to clear Aβ than mouse apoE, we quantified Aβ42 in the CSF in 3-, 7-, and 14-month-old APP-KI, APP-KI/apoE4-KI, and APP-KI/apoE3-KI mice (**Fig. 2A-C**). Approximately 2000 pg/mL of Aβ42 was detected in 3-month-old apoE3 and apoE4 mice. Aβ42 levels in APP-KI mice were slightly lower than in mice expressing human apoE, but there were no significant differences between them (**Fig. 2A**). At 7 months old, the levels of Aβ42 in apoE4 and apoE3 mice were higher than in APP-KI mice, but these differences were also not significant (**Fig. 2B**). However, we found a clear difference in Aβ42 levels in the CSF among the three mice models at 14 months of age (**Fig. 2C**). Aβ42 levels in the CSF were significantly lower in APP-KI mice than in apoE4 ($p < 0.05$) and in apoE3 ($p < 0.0001$) mice. Furthermore, Aβ42 levels in the CSF in apoE4 mice were also significantly lower than in apoE3 mice ($p < 0.01$). To confirm the effect of human apoE in middle adult mice, we collected CVF from 6- to 7-month-old mice and quantified Aβ42 levels (**Fig. 2D**). We detected over 1500 pg/mL and approximately 1000 pg/mL of Aβ42 in the CVF in apoE3 and apoE4 mice, respectively. The amount of Aβ42 in the CVF in APP-KI mice was less than 500 pg/mL. The level of Aβ42 in the CVF in APP-KI mice was significantly lower than in apoE4 ($p < 0.01$) and apoE3 ($p < 0.0001$) mice. Aβ42 levels in the CVF in apoE4 mice was significantly lower than in apoE3 mice ($p <0.01$). The levels of Aβ42 in the CSF and CVF have an almost inverse relationship with Aβ42 levels in the brain parenchyma in similar-aged (5- and 9-month-old) mice (**compare Fig. 2B and D with Fig. 1B and C**).

The level of Aβ42 in the CSF decreased with age in all of the mouse models examined (**Fig. 2A-C**), but apoE3 mice had higher levels of Aβ42 than apoE4 and APP-KI mice at the adult and aged stages. This indicated that human apoE had a higher ability for clearing Aβ42 than mouse apoE from the brain parenchyma into the CSF, at least from the middle adult- to the early-aged stages. The magnitude for Aβ42 clearance was stronger in apoE3 than in apoE4 mice. This finding is consistent with a previous observation (**Castellano et al., 2011**), although discrepancies with regard to the isoform-dependency of apoE levels in the CSF persist controversial (**Riddell et al., 2008; Wildsmith et al., 2012**). Aβ accumulation in the brain of 9-

month-old APP-KI mice may be caused by the low Aβ clearance ability of mouse apoE (**Fagan et al., 2002**). However, the low Aβ clearance activity of mouse apoE continued in these animals until they were at least 14 months old, and Aβ levels in the brain of APP-KI mice did not increase throughout aging (5 months to 21 months old). Therefore, in terms of the ability of only apoE to clear Aβ42 from the brain, it may be difficult to explain how the accumulation of Aβ42 increases linearly in the brain of apoE4 mice during the aging process, and how the level of Aβ42 dramatically increased in late-aged (21-month-old) apoE3 mice.

To resolve these issues, we first investigated brain apoE levels in 13- and 21-month-old mice (**Fig. 3**). However, a previous study shows no differences between apoE3 and apoE4 turnover in the brains of young adult (3.5-month-old) mice (**Wildsmith et al., 2012**). Human apoE expression was examined by immunoblotting using brain lysates from apoE3 and apoE4 mice and an antibody specific for human apoE. The level of brain apoE3 decreased in aged (13-month-old) mice and was significantly lower in 21-month-old mice than in age-matched apoE4 mice. The levels of APP did not change significantly (**Fig. 3A**), suggesting a specific decrease in apoE3. The decrease in apoE3 in the aged mouse brain may trigger the rapid increase in Aβ accumulation in the brain in 21-month-old apoE3 mice, even though apoE3 has a better ability for clearing brain Aβ than apoE4. However, we cannot exclude other possibilities, such as pleiotropic effects by human *APOE* gene expression, which may increase brain Aβ42 levels in mice that express human apoE. Thus, we next analyzed changes in gene expression in aged mouse brains in the presence or absence of human apoE expression.

### *3.2 Characteristic change in gene expression in apoE3 and apoE4 mice models*

To determine the factors responsible for differences in brain Aβ accumulation between apoE3 and apoE4 in early- (13-month-old) and late-aged (21-month-old) mice, we performed RNA sequencing analysis in the brains of APP-KI, apoE3, and apoE4 mice (**Figs. 4 and 5; Supplementary Table 1)**.

First, we analyzed the gene profiles of 13-month-old apoE3 and apoE4 mice, and compared them to the gene profiles of age-matched APP-KI mice (**Figs. 4A and 5A**). We identified 196 genes with altered expression in either apoE3 or apoE4 mice versus APP-KI mice. Of these, the expression of 58 genes was specifically changed in apoE3 mice, while the expression of 49 genes was altered in apoE4 mice. Of the 89 remaining genes found to have common alterations in expression in both apoE3 and apoE4 mice, 82 genes were downregulated and six genes were upregulated in both types of mice. One gene was upregulated in ApoE4 mice but was downregulated in ApoE3 mice. These results indicate that the majority of genes were downregulated in 13-month-old mice in the presence of human apoE but not in the presence of mouse apoE (**Figs. 4A and 5A, Supplementary Table 1**). GO enrichment analysis revealed

that the annotation of genes that specifically changed their expression in apoE3 mice largely belonged to "gene transcription by RNA polymerase II" and "immune system" (**Supplementary Fig. S1A**). Genes for "immune response" also assumed top ranking in apoE4 mice (**Supplementary Fig. S1B**). The annotation of genes that were commonly changed in both apoE3 and apoE4 mice belonged to "cytokines production", "immune response", and "gene transcription by RNA polymerase II" (**Supplementary Fig. S1C**). GO enrichment analysis suggested that alterations in gene expression were related mostly to the "immune system" in mice harboring the human *apoE* gene.

More changes in gene expression were observed in 21-month-old than in 13-month-old mice (**Figs. 4B and 5B**). We identified 387 genes with altered expression in either apoE3 or apoE4 mice versus APP-KI mice. There were 267 specific genes that exhibited changes in expression in apoE3 mice, while 66 genes showed altered expression in apoE4 mice. Furthermore, 54 genes exhibited changes in gene expression that were common to both apoE3 and apoE4 mice, of which 39 genes were upregulated and 15 genes were downregulated. One gene was upregulated in apoE4 mice but was downregulated in apoE3 mice. When compared with 13-month-old mice, these results indicate that many genes were upregulated at 21 months of age in the presence of human apoE (**Figs. 4B and 5B, Supplementary Table 1**). GO enrichment analysis revealed the annotation of genes that had changed in 21-month-old mice. ApoE3 mice showed specific changes in the expression of genes for "protein translation", "mitochondrial function", "endoplasmic reticulum function", and "ATP synthesis" (**Supplementary Fig. S1D**). ApoE4 mice showed specific changes in the expression of genes for "cell surface proteins" and "synapse components" **(Supplementary Fig. S1E)**. The annotation of genes that were commonly changed in both apoE3 and apoE4 mice belonged to "actin function", "synapse formation", and "lipid metabolism" (**Supplementary Fig. S1F**). GO enrichment analysis indicated that there were changes in gene expression related to "glial cell function" in mice carrying the human *apoE* gene.

Among the genes whose expression was significantly altered in mice that harbored human apoE, we focused on 12 genes that exhibited changes in their expression in a human apoE isoform-dependent manner in 13- and 21-month-old mice (indicated with red letters in **Supplementary Table 1**), and whose changes in expression and possible functions are summarized in **Table 1 for (A) 13-month-old and (B) 21-month-old mice**, and with MA plot (**Fig. 5**).

The following is a summary of genes whose expression had changed in 13-month-old mice. [1] The *Sgk1* gene encodes serum-/-glucocorticoid kinase 1 (SDG1) and was downregulated in apoE3 mice. [2] The *Arc* gene encodes the activity-regulated cytoskeleton-associated protein (Arc) and was downregulated in both apoE3 and apoE4 mice. [3] The *Trem2*

gene encodes a receptor type I membrane protein and was downregulated in both apoE3 and apoE4 mice. [4] The *Atp5h* gene is embedded in the intron of the *KCTD2* gene (*ATP5H/KCTD2* locus). The expression of these genes was downregulated in apoE4 mice. [5] The *Ide* gene encodes an insulin-degrading enzyme, which is also known to degrade Aβ (**Qiu & Folstein 2006**). That gene was downregulated in apoE4 mice. [6] The expression of *Vgf*, whose name is non-acronymic and indicates "nerve growth factor inducible", was upregulated in apoE4 mice (**Table 1A, Fig. 5A**).

The following are genes whose expression had changed in 21-month-old mice. [7] The *Ndrg2* (*N-myc down-regulated gene family member 2*) gene encodes α/β-hydrase fold protein and was upregulated in apoE4 mice. [8] The *Abca1* gene encodes ATP-binding cassette transporter 1 that plays an important role in cholesterol efflux. *Abca1* expression was upregulated in apoE4 mice. [9] The *Timp3* gene encodes a metalloprotease inhibitor, TIMP3. Upregulation of *TIMP3* expression was observed in apoE4 mice. [10] The *Apod* gene encodes apolipoprotein D (apoD) and was upregulated in apoE4 mice. [11] *Calr* gene encodes calreticulin, an endoplasmic reticulum resident protein 60. This gene was upregulated in apoE3 mice. [12] The *Vegfa* gene encodes the vascular endothelial growth factor A (VEGF-A) and was upregulated in apoE3 mice. [3] The *Trem2* gene was downregulated in apoE3 mice, and [6] *Vgf* gene expression was upregulated in apoE3 mice (**Table 1B, Fig. 5B**).

### *3.3 Confirmation of changes in gene expression using RT-qPCR analysis*

We confirmed changes in gene expression in 12 genes (e.g., *Atp5h, Ide, Trem2, Arc,* shown in Table1) through quantification with RT-qPCR (**Fig. 6**). The *Atp5h* gene was significantly downregulated in 13-month-old apoE4 but not apoE3 mice. The *Atp5h* gene was significantly downregulated in both 21-month-old apoE3 and apoE4 mice, the magnitude of which was greater in apoE4 than in apoE3 mice. The magnitude of *Atp5h* expression in 21-month-old mice was also stronger than in 13-month-old mice, indicating that this regulation was age dependent. The downregulation of *Ide* in 13-month-old apoE4 mice was confirmed with RT-qPCR. *Ide* expression showed a trend of downregulation in 21-month-old apoE4 ($p$ =0.089) and apoE3 ($p$ = 0.053) mice. The *Trem2* gene was significantly downregulated with the exception of 21-month-old apoE4 mice. These results of three genes coincided with data from RNA-seq analysis. Taken together, these three genes, *Atp5h, Ide,* and *Trem2*, were downregulated in the presence of human apoE, and the magnitude of this downregulation is likely to be greater in apoE4 than in apoE3 mice.

In contrast to these three genes, the *Arc* gene was strongly downregulated in 13-month-old apoE3 and apoE4 mice, a finding that was consistent with results from the RNA-seq data analysis. *Arc* expression may be regulated in an age-dependent manner in the presence of

human apoE without isoform specificity. Overall, the expression profiles of the four genes assessed by RT-qPCR completely matched changes in expression identified by RNA-seq analysis in both apoE isoforms and age dependency.

## 4. Discussion

In this study, we revealed the effects of human apoE3 and apoE4 isoforms on Aβ accumulation through the life span and compared gene expression profiles in the brain with mouse apoE at early (13-month-old) and late (21-month-old)-aged stages in double-KI mouse models. In AD pathobiology, there are a variety of reports on the functional differences of apoE isoforms in cells and animals. However, the role of apoE4, the strongest genetic risk factor for AD, remains controversial with regard to the pathogenesis and progression of AD (**Martens et al., 2022**). One reason for this controversy may be the lack of factors for aging in animals because aging itself is the greatest risk factor for AD. The aging process includes various and complex molecular alterations such as epigenetic modifications of genes, post-translational modifications of proteins, and changes in the composition of membrane lipids. Moreover, this complexity may be intertwined in the individual aging process because of the pleiotropic nature of the *apoE* gene (**Hou et al., 2019**). To understand the complex roles of human apoE in brain Aβ burden during aging, we first revealed the process of Aβ accumulation in the brain of three mouse models, APP-KI/apoE4 (apoE4), APP-KI/apoE3 (apoE3), and APP-KI/mouse apoE (APP-KI), throughout their aging process. The analysis was performed in young adult (3-month-old), middle adult (5- and 9-month-old), and in early (13-month-old) and late (21-month-old)-aged female mice.

Since APP-KI ($APP^{NL\text{-}G\text{-}F/NL\text{-}G\text{-}F}$) mice exhibit longevity without the influence of transgenes and because Aβ pathology in these mice is similar to that in the brain of patients with AD (**Saito et al., 2014; Saito & Saido 2018**), we analyzed brain Aβ accumulation throughout the aging process and revealed the distinct process in Aβ42 accumulation among mouse models that express human apoE3, human apoE4, and mouse apoE. Our study took the aging factor into account to understand the roles of apoE isoforms in the progression of Aβ accumulation. In humans, apoE4 plays a significant role in early and middle onset AD (**Raber et al., 2004; Spinney et al., 2014)**, which is consistent with our data that showed that Aβ42 accumulates linearly in the brain with age in apoE4 mice. Interestingly, brain Aβ42 levels were dramatically increased in late-aged (21-month-old) apoE3 mice. This suggests that apoE3 may be a risk factor for the progression of late-onset AD, and that apoE4, as described elsewhere, is a major risk factor for the progression of AD pathology in the earlier stages of aging rather than apoE3. The higher risk of apoE4 during the middle adult to aged stages may be attributed to a weaker Aβ clearance ability of apoE4 than apoE3 (**Castellano et al., 2011**). In our study, we propose

that apoE3 is a novel risk factor in late-aged (21-month-old) mice, which may be caused by a reduction in apoE3 protein in the aged brain.

To further understand the influence of apoE isoforms on Aβ accumulation in the brain of aged individuals, we performed gene expression analysis in three mouse models at the early (13-month-old) and late (21-month-old)-aged stages, and identified genes whose expression significantly changed in an apoE isoform-dependent and -independent (or human apoE-dependent) manner, and in an age-dependent and -independent manner. We selected twelve genes whose expression was strongly and significantly changed. This included genes that are reported as being risk factors for, or that are relevant to, AD (**Table 1**). Among these twelve genes, the expression profiles of the following four genes (*Atp5h*, *Ide*, *Trem2*, and *Arc*) were confirmed with RT-qPCR.

*Atp5h* expression was downregulated in both apoE3 and apoE4 mice, and the magnitude of this change was stronger in apoE4 than in apoE3 mice. The *Atp5h* gene encodes ATP synthase H+ transporting mitochondrial Fo, which is a component of Complex V and plays an important function in ATP generation. This gene is embedded in the intron of the *Kctd2* gene, which encodes potassium channel tetramerization domain-containing protein 2; a genome-wide association study (GWAS) linked the *ATP5H/KCTD2* locus with AD risk (**Boada et al., 2014**). Since this locus is closely associated with energy production in mitochondria, the downregulation of the *Atp5h* gene in the presence of human apoE may therefore be associated with the impairment of mitochondrial functions in neurons, which increases Aβ load in aged individuals. Indeed, mitochondrial function is usually decreased in the brain of AD patients (**Ridge & Kauwe 2018; Swerdlow et al., 2014**). Downregulation of the *Atp5h* gene in the presence of human apoE, especially the apoE4 isoform, may cause Aβ load in the brain to increase with age.

The *Ide* gene encodes IDE, which degrades insulin and Aβ (**Qiu & Folstein 2006**). In patients carrying the apoE4 allele, IDE expression is high in the middle stage of AD (Braak stages 3–4) and is reduced in the later stages of AD (Braak stages 5–6) (**Delikkaya et al., 2019**). Our data show that IDE expression was significantly downregulated in early-aged (13-month-old) mice in the presence of apoE4. The downregulation tended to be continued in both 21-month-old apoE3 and apoE4 mice. Although IDE acts bidirectionally to advance AD by degrading brain insulin, and to suppress AD by degrading Aβ, insulin degradation rather than Aβ lysis is thought to be the main function of IDE (**Delilkkaya et al., 2019**). Secreted Aβ is degraded mainly by neprilysin rather than by IDE (**Iwata et al., 2001; Saito et al., 2005**). Therefore, the downregulation of *Ide* gene expression may be associated with the intracellular increase in Aβ, which is also toxic to mitochondrial function in neurons (**Martens et al., 2022**).

The *Arc* gene encodes Arc, which regulates the endosomal pathway for Aβ generation, and the genetic depletion of Arc reduces Aβ load in the APP-Tg mouse model of AD (**Wu et al., 2011**). A gene polymorphism in *Arc* is associated with a reduced risk of AD (**Landgren et al., 2012**), and Arc-expressing cells are decreased in the cortex in a mouse model of AD (**Wegenast-Braun et al., 2009**). In the current study, *Arc* gene expression was downregulated in early-aged (13-month-old) apoE3 and apoE4 mice. This downregulation was not observed in late-aged (21-month-old) mice. The decrease in ARC in early-aged mice may be a response to the increasing Aβ burden in the presence of human apoE, and the loss of this response in late-aged mice may contribute to the increase in Aβ accumulation in the mouse brain.

The *Trem2* gene encodes a receptor type I membrane protein that associates with TYRO protein kinase-binding protein (TYROBP). This protein complex activates microglia, increasing phagocytosis and cytokine production, which are thought to be protective reactions against neurotoxic Aβ accumulation. TYROBP associates with TREM2 and a decrease in TYROBP increases Aβ accumulation in the brain (**Audrain et al., 2021**). Therefore, reduced function and/or expression of TREM2 is associated with a risk of AD progression (**Guerrreiro et al., 2013**). Downregulation of *Trem2* expression in apoE3 and apoE4 mice at 13 and 21 months of age suggests a reduction in protective reactions by microglia in the presence of human apoE. Our GO analysis suggests that genes associated with glial cell functions are downregulated in human apoE-expressing aged mice.

Eight other genes with significantly altered expression, as assessed by RNA-seq analysis, have also been linked with AD. In mice, the consumption of a high-fat diet increases *Sgk1* gene expression, which leads to neurodegeneration along with tau pathology (**Elahi et al., 2021**). The *Vgf* gene is a key regulator of AD; its expression is increased in the x5 FAD mouse model, which decreases Aβ levels significantly in the brain (**Beckmann et al., 2020**). The *Ndrg2* gene is upregulated in late-onset AD brains (**Michelmore et al., 2004**), but its roles in AD pathology remain unclear. The *Abca1* gene is found by genome-wide AD linkage studies and is linked to the risk of late-onset AD (**Sundar et al., 2007**). Lack of ABCA1, a cholesterol transporter in the brain, is associated with a decrease in apoE together with increased Aβ deposition in the brain (**Hirsch-Reinshagen et al., 2005; Koldamova et al., 2005; Wahrle et al., 2005**). *Timp3* encodes TIMP3, which inhibits the cleavage of APP. The levels of apoE receptor 2 and TIMP3 are increased in the brain of AD patients and in APP-Tg mice **(Hoe et al., 2007**). The *Apod* gene is upregulated in AD but not in frontotemporal dementia (**Bhatia et al., 2019**). ApoD may respond to cellular stresses in the degenerative brain **(Dassati et al., 2014**). Loss of *apod* increases brain amyloid plaques in the APP-PS1 mouse model of AD (**Li et al., 2015**). Furthermore, apoD, together with apoE2 and apoE3 but not apoE4, plays an important role in the transfer of peroxidated lipids produced by high levels of neuronal ROS (reactive oxygen

species) into glia (**Liu et al., 2017; Moulton et al., 2021**). The *Calr* gene encodes calreticulin, which regulates gene transcription mediated by nuclear hormone receptors (**Dey & Matsunami 2011**). Calreticulin has been identified as a negative biomarker in the serum of patients with AD. Serum calreticulin levels decrease as AD progresses (**Lin et al., 2014**). The *Vegfa* gene encodes VEGF-A, which is involved in the development of AD. The genetic variants of the *vegfa* gene are reported to be strong protective factors against AD (**Petrelis et al., 2022**).

Interestingly, the expression of many genes was altered in the presence of human apoE, in either apoE3 or apoE4 mice at 13 and 21 months old. Some of these genes that we have described here may contribute to the progressive accumulation of Aβ in the brain at early- and late-aged stages in an apoE4- and/or apoE3-dependent manner. Among 12 selected genes, we identified four genes and summarized their possible functions as candidates that may increase Aβ burden in the presence of human apoE. Further biochemical and/or biological analyses of these genes may offer insight into the molecular functions of human apoE in the progression of sporadic AD with an increased Aβ burden.

**5. Conclusions**

Brain Aβ42 levels were significantly lower in both apoE4 and apoE3 mice than in APP-KI mice that did not express human apoE at 9 months of age. The accumulation of Aβ42 was followed by a linear increase in Aβ42 in 5-month-old apoE4 mice. Aβ42 levels increased dramatically after 13-month-old in apoE3 mice and reached the level of Aβ42 found in late-aged (21-month-old) apoE4 mice. APP-KI (5- to 21-month-old) mice had a constant level of Aβ42 and there was no increase in Aβ42 during the aging process. Taken together, human apoE suppresses Aβ42 accumulation in the young- and middle-adult stages, but increases it in the early- and late-aged stages.

In the middle adult and early-aged stages, the levels of Aβ42 in the CSF and CVF were significantly higher in apoE3 mice than in apoE4 mice, suggesting a weaker clearance ability of Aβ from brain parenchyma in apoE4 mice at these stages. However, in 21-month-old mice, the level of apoE3 protein in the brain was lower than that of apoE4 protein, which may explain the rapid increase in Aβ42 levels in late-aged apoE3 mice. Throughout the aging process, many genes must interact together to express AD pathology including Aβ accumulation in the brain. To identify the genes that are regulated by human apoE isoforms in aged individuals, we examined gene expression profiles in the brains of 13- and 21-month-old mice. We found several interesting genes whose expression we classified into the apoE isoform-dependent and the human apoE-dependent categories, together with aging factors. Although some of these genes are known to be associated with AD, they have not been sufficiently analyzed to determine whether their expression is apoE and/or age dependent.Among the genes examined,

we identified four gene candidates that influence Aβ load in the presence of human apoE. Altered regulation of these genes in the presence of the human apoE and during the progression of aging may generate distinct processes of Aβ accumulation in the brain.

---

**Submission declaration and verification**

The authors declare that this work has not been published previously, nor is it under consideration for publication elsewhere. All authors approved the submission of the manuscript to this journal.

**Disclosure statement**

All authors report no conflict of interest.

**Acknowledgments**

We thank all laboratory members who contributed through helpful suggestions and discussion. This work was supported in part by Japan Agency for Medical Research and Development (21dk0207059s0101 to T.S.) and The Naito Foundation (S.H.). We thank Dr. Sam Gandy for supplying APP antibody, and Mitsubishi Kagaku, Co. Ltd., and Dr. Shinobu C. Fujita for supplying apoE-KI mice.

**Author contributions**

**Honda, K:** Formal analysis, Investigation, Original draft. **Saito, Y:** Conceptualization, Methodology, Formal analysis, Writing: review & editing. **Saito, H:** Methodology, Formal analysis. **Toyoda, M:** Formal analysis, Investigation. **Abe, R:** Formal analysis, Investigation. **Saito, T:** Methodology, Writing: review & editing. **Saido, T.C.:** Methodology, Writing: review & editing. **Michikawa, M:** Methodology, Writing: review & editing. **Taru, H:** Methodology, Writing: review & editing. **Sobu, Y:** Formal analysis, Methodology, Writing: review & editing, Funding acquisition. **Hata, S:** Formal analysis, Methodology, Writing: review & editing, Funding acquisition, **Nakaya, T:** Methodology, Writing: review & editing. **Suzuki, T:** Conceptualization, Methodology, Original draft, Writing: review & editing, Supervision, Funding acquisition, Project administration.

**References**

2021 Alzheimer's disease facts and figure. https://www.alz.org/media/Documents/ alzheimers-facts-and-figures.pdf

Audrain, M., Haure-Mirande, J-V., Mleczko, J., Wang, M., Griffin, J. K., St. George-Hyslop, P. H., Fraser, P., Zhang, B., Gandy S., Ehrlich, M. E., 2021. Reactive or transgenic increase in microglial TYROBP reveals a TREM2-independent TYROBP-APOE link in wild-type and Alzheimer's-related mice. Alzheimers Dement. 17 (2),149-163. doi:10.1002/alz.12256.

Beckmann, N. D., Lin, W-J., Wang, M., Cohain, A. T., Charney, A. W., Wang, P., Ma, W., Wang, Y-C., Jiang, C., Audrain, M., Comella, P. H., Fakira, A. K., Hariharan, S. P., Belbin, G. M., Girdhar, K., Levey, A. I., Seyfried, N T., Dammer, E. B., Duong, D., Lah, J. J., Haure-Mirande, J-V., Shackleton, B., Fanutza, T., Blitzer, R., Kenny, E., Zhu, J., Haroutunian, V., Katsel, P., Gandy, S., Tu, Z., Ehrlich, M. E., Zhang, B., Salton, S. R., Schadt, E. E., 2020. Multiscale causal networks identify VGF as a key regulator of Alzheimer's disease. Nat. Commun. 11 (1), 3942 doi: 10.1038/s41467-020-17405-z.

Benilova, I., Karran, E, De Strooper, B., 2012. The toxic Aβ oligomer and Alzheimer's disease: an emperor in need of clothes. Nat. Neurosci. 15 (3), 349-357. doi: 10.1038/nn.3028.

Bhatia, S., Kim, W. S., Shepherd, C. E., Halliday, G. M., 2019. Apolipoprotein D upregulation in Alzheimer's disease but not frontotemporal dementia. J. Mol. Neurosci. 67 (1), 125-132. doi. 10.1007/s12031-018-1217-9.

Boada, M., Antúnez, C., Ramírez-Lorca, R., DeStefano, A. L., González-Pérez, A., Gayán, J., López-Arrieta, J., Ikram, M. A., Hernández, I., Marín, J., Galán, J. J., Bis, J. C., Mauleón, A., Rosende-Roca, M., Moreno-Rey, C., Gudnasson, V., Morón, F. J., Velasco, J., Carrasco, J. M., Alegret, M., Espinosa, A., Vinyes, G., Lafuente, A., Vargas, L., Fitzpatrick, A. L., Alzheimer's Disease Neuroimaging Initiative; Launer, L., Sáez, M. E., Vázquez, E., Becker, J. T., López, O. L., Serrano-Rios, M., Tárraga, L., van Duijn, C. M., Real, L. M., Seshadri, S., Ruiz, A., 2014. ATP5H/KCTD2 locus is associated with Alzheimer's disease risk. Mol. Psych., 19 (6), 682-687. doi: 10.1038/mp.2013.86.

Castellano, J. M., Kim, J., Stewart, F. R., Jiang, H., DeMattos, R. B., Patterson, B. W., Fagan, A. M., Morris, J. C., Mawuenyega, K. G., Cruchaga, C., Goate, A. M., Bales, K. R., Paul, S. M., Bateman, R. J., Holtzman, D. M., 2011. Human apoE isoforms differentially regulate brain amyloid-β peptide clearance. Sci. Transl. Med., 3 (89): 89ra57. doi: 10.1126/scitranslmed.3002156.

Cole, S. L., Vassar, R., 2008. The role of amyloid precursor protein processing by BACE1, the β-secretase, in Alzheimer's disease pathophysiology. J. Biol. Chem. 283 (44), 29621-29625. doi: 10.1074/jbc.R800015200.

Corder, E. H., Sunders, A. M., Strittmatter, W. J., Schmechel, D. E., Gaskell, P. C., Small, G. W., Roses, A. D., Haines, J. L., Pericak-Vance, M. A., 1993. Gene dose of apolipoprotein E type 4 allele and the risk of Alzheimer's disease in late onset families. Science 261 (5123), 921-923. doi: 10.1126/science.8346443.

Dassati, S., Waldner, A., Schweigreiter, R., 2014, Apolipoprotein D takes center stage in the stress response of the aging and degenerative brain. Neurobiol. Aging. 35 (7),1632-1642. doi:10.1016/j.neurobiolaging.2014.01.148.

Delikkaya, B., Moriel, N., Tong, M., Gallucci, G., de la Monte, S. M., 2019. Altered expression of insulin-degrding enzyme and regulator of calcineurin in the rat intracerebral streptozotocin model and human apolipoprotein E-ε4-associated Alzheimer's disease. Alzheimers Dement (Amst). 11, 392-404. doi: 10.1016/j.dadm.2019.03.004.

Dey, S., Matsunami, H., 2011. Calreticulin chaperones regulate functional expression of vomeronasal type 2 pheromone receptors. Proc. Natl. Acard. Sci. U.S.A. 108 (40), 16651-16656. doi: 10.1073/pnas.1018140108.

Di Fede, G., Catania, M., Morbin, M., Rossi, G., Suardi, S., Mazzoleni, G., Merlin, M., Giovagnoli, A. R., Prioni, S., Erbetta, A., Falcone, C., Gobbi, M., Colombo, L., Bastone, A., Beeg, M, Manzoni, C., Francescùcci, B., Spagnoli, A., Cantu, L., Del Favero, E., Levy, E., Salmona, M.,Tagliavini, F., 2009. A recessive mutation in the APP gene with dominant-negative effect on amyloidogenesis. Science 323 (5920), 1473-1477. doi: 10.1126/science.1168979.

Elahi, M., Motoi, Y., Shimonaka, S., Ishida, Y., Hioki, H., Takanashi, M., Ishiguro, K., Imai, Y., Hattori, N., 2021. High-fat diet-induced activation of SGK1 promotes Alzheimer's disease-associated tau pathology. Hum. Mol. Gennet. 30(18), 1693-1710. doi: 10.1093/hmg/ddab115.

Fagan, A. M., Watson, M., Parasadanian, M., Bales, K. R., Paul, S. M. Holtzman, D. M., 2002. Human and murine apoE markedly alters Aβ metabolism before and after plaque formation in a mouse model of Alzheimer's disease. Neurobiol. Dis. 9 (3), 305-318. doi: 10.1006/nbdi.2002.0483.

Guerreiro, R., Wojtas, A., Bras, J., Carrasquillo, M., Rogaeva, E., Majounie, E., Cruchaga, C., Sassi, C., Kauwe, J. S. K., Younkin, S., Hazrati, L., Collinge, J., Pocock, J., Lashley, T., Williams, J., Lambert, J-C., Amouyel, P., Goate, A., Rademakers, R., Morgan, K., Powell, J., St. George-Hyslop, P., Singleton, A., Hardy, J. Alzheimer Genetic Analysis Group., 2013. TREM2 variants in Alzheimer's disease. N. Engl. J. Med. 368 (2), 117—127. doi: 10.1056/NEJMoa1211851.

Hamanaka, H., Katoh-Fukui, Y., Suzuki, K., Kobayashi, M., Suzuki, R., Motegi, Y., Nakahara, Y., Takeshita, A., Kawai, M., Ishiguro, K., Yokoyama, M., Fujita, S. C., 2000. Altered cholesterol metabolism in human apolipoprotein E4 knock-in mice. Human. Mol. Genet. 9 (3), 353-361. doi: 10.1093/hmg/9.3.353.

Hashimoto, T., Serrano-Pozo, A., Hori, Y., Adams, K. W., Takeda, S., Baneriji, A. O., Mitani, A., Joyner, D., Thyssen, D. H., Bacskai, B. J., Frosch, M. P., Spires-Jones, T. L., Finn, M. B., Holtzman D. V., Hyman, B. T., 2012. Apolipoprotein E, especially apolipoprotein E4, increases the oligomerization of amyloid β peptide. J. Neurosci. 32 (43), 15181-15192. doi: 10.1523/JNEUROSCI.1542-12.2012.

Hirsch-Reinshagen, V., Maia, L. F., Burgess, B. L., Blain, J-F., Naus, K. E., Mclsaac, S. A., Parkinson, P. F., Chan, J. Y., Tansley, G. H., Hayden, M. R., Poirier, J., Van Nostrand, W., Wellington, C. L., 2005. The absence of ABCA1 decreases soluble ApoE levels but does not diminish amyloid deposition in two murine models of Alzheimer disease. J. Biol. Chem. 280(52), 43243-43256. doi: 10.1074/jbc.M508781200.

Hoe, H-S., Cooper, M. J., Burns, M. P., Lewis, P. A., van der Brug, M., Chakraborty, G., Cartagena, C. M., Pak, D. T. S., Cookson, M. R., Rebeck, G. W., 2007. The metalloprotease

inhibitor TIMP-3 regulates amyloid precursor protein and apolipoprotein E receptor proteolysis. J. Neurosci. 27 (40), 10895-10905. doi: 10.1523/JNEUROSCI.3135-07.2007.

Holtzman, D. M., Bales, K. R., Wu, S., Bhat, P., Parsadanian, M., Fagan, A. M., Chang L. K., Sun, Y., Paul, S. M., 1999. Expression of human apolipoprotein E reduces amyloid-β deposition in mouse model of Alzheimer's disease. J. Clinic. Invest. 103 (6), R15-21. doi. 10.1172/JCI6179

Hou, Y., Dan, X., Babbar, M., Wei, Y., Hasselbalch, S. G., Croteau, D. L., Bohr, V. A., 2019. Aging as a risk factor for neurodegenerative disease. Nat. Rev. Neurol. 15 (10), 565-581. doi: 10.1038/s41582-019-0244-7.

Iwata, N., Tsubuki, S., Takaki, Y., Shirotani, K., Lu, B., Gerard, N. P., Gerard, C., Hama, E., Lee, H. J., Saido, T. C., 2001. Metabolic regulation of brain Aβ by neprilysin. Science 292 (5521), 1550-1552. doi: 10.1126/science.1059946.

Jonsson, T., Atwal, J. K., Steinberg, S., Snaedal, J., Jonsson, P. V., Bjornsson, S., Stefansson, H., Sulem, P., Gudbjartsson, D., Maloney, J., Hoyte, K., Gustafson, A., Liu, Y., Lu, Y., Bhangale, T., Graham, R. R., Huttenlocher, J., Bjornsdottir, G., Andreassen, O. A., Jönsson, E. G., Palotie, A., Behrens, T. W., Magnusson, O. T., Kong, A., Thorsteinsdottir, U., Watts, R.J., Stfansson, K., 2012. A mutation in APP protects against Alzheimer's disease and age-related cognitive decline. Nature 488 (7409), 96-99. doi: 10.1038/nature11283.

Kimura, A., Hata, S., Suzuki, T., 2016. Alternative selection of β-site APP-cleaving enzyme 1 (BACE1) cleavage sites in amyloid β-protein precursor (APP) harboring protective and pathogenic mutations within the Aβ sequence. J. Biol. Chem. 291(46), 24041-24053. doi: 10.1074/jbc.M116.744722.

Koldamova, R., Staufenbiel, M., Lefterov, I., 2005. Lack of ABCA1 considerably decreases brain ApoE level and increases amyloid deposition in APP23 mice. J. Biol. Chem. 280 (52), 43224-43235. doi: 10.1074/jbc.M504513200.

Kondo, M., Shiono, M., Itoh, G., Takei, N., Matsushima, T., Maeda, M., Taru, H., Hata, S., Yamamoto, T., Saito, Y., Suzuki, T., 2010. Increased amyloidogenic processing of transgenic human APP in X11-like deficient mouse brain. Mol. Neurodegener. 5:35. doi: 10.1186/1750-1326-5-35.

Landgren, S., von Otter, M., Palmér, M. S., Zetterström, C., Nilsson, S., Skoog, I., Gustafson, D. R., Minthon, L., Wallin, A., Andreasen, N., Bogdanovic, N., Marcusson, J., Blennow, K., Zetterberg, H., Kettunen, P., 2012. A novel ARC gene polymorphism is associated with reduced risk of Alzheimer's disease. J. Neural. Ttansm (Vienna). 119 (7), 833-842. doi: 10.1007/s00702-012-0823-x.

Laemmli, U. K.,1970. Cleavage of structural proteins during the assembly of the head of bacteriophage T4. Nature 227 (5259), 680-685. doi: 10.1038/227680a0.

Li, H., Ruberu, K., Muñoz, S. S., Jenner, A. M., Spiro, A., Zhao, H., Rassart, E., Sanchez, D., Ganfornina, M, D., Karl, T., Garner, B., 2015. Apolipoprotein D modulates amylpid pathology in APP/PS1 Alzheimer's disease mice. Neurobiol. Aging 36 (5), 1820-1833. Doi:10.1016/j.neurobiolaging.2015.02.010

Lin, Q., Cao, Y., Gao, J., 2014. Serum calreticulin is a negative biomarker in patients with Alzheimer's disease. Int. J. Mol. Sci. 15 (12), 21740-21753. doi:10.3390/ijms151221740.

Liu, L., Duff, K., 2008 A technique for serial collection of cerebrospinal fluid from the cisterna magna in mouse. *J. Vis. Exp.* 21: 960 (http://www.jove.com/index/Details.stp?ID=960) doi: 10.3791/960 pmid: 19066529

Liu, L., MacKenzie, K. R., Putluri, N., Maletić-Savatić, M., Bellen, H. J., 2017 The glia-neuron lactate shuttle and elevated ROS promote lipid synthesis in neurons and lipid droplet accumulation in glia via apoE/D. Cell Metab. 26 (5), 719-737. e6. doi:10.1016/j.cmet.2017.08.024.

Love, M. I., Huber, W., Anders, S., 2014 Moderated estimation of fold change and dispersion for RNA-seq data with DESeq2. Genome Biol. 15 (12):550. doi. 10.1186/s13059-014-0550-8.

Martens, Y., A., Zhao, N., Liu, C-C., Kanekiyo, T., Yang, A. J., Goate, A., M., Holtzman, D., M., Bu, G., 2022. ApoE cascade hypothesis in the pathogenesis of Alzheimer's disease and related dementias. Neuron 110 (8), 1304-1317. doi: 10.1016/j.neuron.2022.03.004.

Mitchelmore, C., Büchmann-Møller, S., Rask, L., West, M. J., Troncoso, J. C., Jensen, N. A., 2004. NDRG2: a novel Alzheimer's disease associated protein. Neurobiol. Dis. 16 (1), 48-58. doi: 10.1016/j.nbd.2004.01.003.

Mizumaru, C., Saito, Y., Ishikawa, T., Yoshida, T., Yamamoto, T., Nakaya, T., Suzuki, T., 2009. Suppression of APP-containing vesicle trafficking and production of β-amyloid by AID/DHHC-12 protein. J. Neurochem. 111 (5), 1213-1224. doi: 10.1111/j.1471-4159.2009.06399.x.

Mori, T., Kobayashi M., Town, T., Fujita, S. C., Asano, T., 2003. Increased vulnerability to focal ischemic brain injury in human apolipoprotein E4 knock-in mice. J. Neuropathol. Exp. Neurol. 62 (3), 280-291. doi: 10.1093/jnen/62.3.280.

Moulton, M. J., Barish, S., Ralhan, I., Chang, J., Goodman, L. D., Harland, J. G., Marcogliese, P. C., Johansson, J. O., Ioannou, M. S., Bellen, H. J., 2021. Neuronal ROS-induced glial lipid droplet formation is altered by loss of Alzheimer's disease-associated genes. Proc. Natl. Acard. Sci. U. S. A. 118 (52), e2112095118. doi: 10.1073/pnas.2112095118.

Mullan, M., Crawford, F., Axelman, K., Houlden, H., Lilius, L., Winblad, B., Lannfelt, L., 1992. A pathogenic mutation for probable Alzheimer's disease in the APP gene at N-terminus of β-amyloid. Nat. Genet. 1(5), 345-347. doi: 10.1038/ng0892-345.

Oishi, M., Nairn, A. C., Czernik, A. J., Lim, G. S., Isohara, T., Gandy, S. E., Greengard, P., Suzuki, T., 1997. The cytoplasmic domain of the Alzheimer's amyloid precursor protein is phosphorylated at Thr654, Ser655 and Thr668 in adult rat brain and cultured cells. Mol. Med. 3 (2), 111-123.

Petrelis, A. M., Stathopoulou, M. G., Kafyra, M., Murray, H., Masson, C., Lamont, J., Fitzgerald, P., Dedoussis, G., Yen, F. T., Visvikis-Siest, S., 2022. VEGF-A-related genetic variants protect against Alzheimer's disease. Aging (Albany NY) 14 (6), 2524-2536. doi: 10.18632/aging.203984.

Qiu, W. Q., Folstein, M. F., 2006. Insulin, insulin-degrading enzyme and amyloid-β peptide in Alzheimer's disease: review and hypothesis. Neurobiol. Aging. 27 (2), 190-198. doi:10.1016/j.neurobiolaging.2005.01.004.

Raber, J., Huang, Y., Ashford, J. W., 2004. ApoE genotype accounts for the vast majority of AD risk and AD pathology. Neurobiol. Aging 25 (5), 641-650. doi: 10.1016/j.neurobiolaging.2003.12.023.

Riddell, D. R., Zhou, H., Atchison, K., Warwick, H. K., Atkinson, P. J., Jefferson, J., Xu, L., Aschmies, S., Kirksey, Y., Hu, Y., Wagner, E., Parratt, A., Xu, J., Li, Z., Zaleska, M. M., Jacobsen, J. S., Pangalos, M. N., Reinhart, P. H., 2008. Impact of apolipoprotein E (ApoE) polymorphism on brain apoE levels. J. Neurosci. 28 (45), 11445-11453. doi: 10.1523/JNEUROSCI.1972-08.2008.

Ridge, P. G., Kauwe, J. S. K., 2018. Mitochondria and Alzheimer's disease: the role of mitochondrial genetic varidation. Curr. Genet. Med. Rep. 6 (1), 1-10. doi: 10.1007/s40142-018-0132-2.

Saito, T., Iwata, N., Tsubuki, S., Takaki, Y., Takano, J., Huang, S-M., Suemoto, T., Higuchi, M., Saido, T. C., 2005. Somatostatin regulates brain amyloid β peptide Aβ42 through modulation of proteolytic degradation. Nat. Med. 11 (4), 434-439. doi: 10.1038/nm1206.

Saito, T., Matsuba, Y., Mihira, N., Takano, J., Nilsson, P., Itohara, S., Iwata, N., Saido, T. C., 2014. Single App knock-in mouse models of Alzheimer's disease. Nat. Neurosci. 17 (5), 661-663. doi: 10.1038/nn.3697.

Saito, T., Saido, T. C., 2018. Neuroinflammation in mouse models of Alzheimer's disease. Clin. Exp. Neuroimmunol. 9 (4), 211-218. doi: 10.1111/cen3.12475.

Selkoe, D. J., 2011. Alzheimer's Disease. Cold Spring Harb. Perspect Biol. 3(7), a004457. doi: 10.1101/cshperspect.a004457.

Spinney, L., 2014. Alzheimer's disease: The forgetting gene. Nature 510 (7503), 26-28. doi: 10.1038/510026a.

Sundar, P. D., Feingold, E., Minster, R. L., DeKosky, S. T., Kamboh, M. I., 2007. Gender-specific association of ATP-binding cassette transporter 1 (ABCA1) polymorphisms with the risk of late-onset Alzheimer's disease. Neurobiol. Aging. 28 (6), 856-862. doi: 10.1016/j.neurobiolaging.2006.04.005.

Swerdlow, R. H., Burns, J M., Khan, S. M., 2014. The Alzheimer's disease mitochondrial cascade hypothesis: progress and perspectives. Biochim. Biophys. Acta 1842 (8), 1219-1231. doi: 10.1016/j.bbadis.2013.09.010.

TCW, J., Qian, L., Pipalla, N. H., Chao, M. J., Liang, S. A., Shi, Y., Jain, B. R., Bertelsen, S. E., Kapoor, M., Marcora, E., Dikora, E., Andrews, E. J., Martini, A. C., Karch, C. M., Head, E., Holtzman, D. V., Zhang, B., Wang, M., Maxfield, F. R., Poon, W. W., Goate, A. M., 2022. Cholesterol and matrisome pathways desregulated in astrocytes and microglia. Cell, 185, 2213-2233. Doi: 10.1016/j.cell.2022.05.017.

Thinakaran, G., Koo, E. H., 2008. Amyloid precursor protein trafficking, processing, and function. J. Biol. Chem. 283 (44), 29615-29619. doi: 10.1074/jbc.R800019200.

Tomita, S., Kirino, Y., Suzuki, T., 1998. Cleavage of Alzheimer's amyloid precursor protein (APP) by secretases occurs after O-glycosylation of APP in the protein secretory pathway. Identification of intracellular compartments in which APP cleavage occurs without using toxic agents that interfere with protein metabolism. J. Biol. Chem. 273 (11), 6277-6284. doi: 10.1074/jbc.273.11.6277.

Wahrle, S. E., Jiang, H., Parsadanian, M., Hartman, R. E., Bales, K. R., Paul, S. M., Holtzman, D. M., 2005. Deletion of Abca1 increases Aβ deposition in the PDAPP transgenic mouse model of Alzheimer disease. J. Biol. Chem. 280 (52), 43236-43242. doi: 10.1074/jbc.M508780200.

Wegenast-Braun, B. M., Maisch, A. F., Eicke, D., Radde, R., Herzig, M. C., Staufenbiel, M., Jucker, M., Calhoun, M. E., 2009. Independent effects of intra- and extracellular Aβ on learning-related gene expression. Am. J. Pathol. 175 (1), 271-282. doi:10.2353/ajpath.2009.090044.

Wildsmith, K. R., Basak, J. M., Patterson, B. W., Pyatkivskyy, Y., Kim, J., Yarasheski, K. E., Wang, J. X., Mawuenyega, K. G., Jiang, H., Parsadanian, M., Yoon, H., Kasten, T., Sigurdson, W. C., Xiong, C., Goate, A., Holtzman, D. M., Bateman, R. J., 2012. In vivo human apolipoprotein E isoform fractional turnover rates in the CNS. PLoS ONE 7 (6), e38013. doi: 10.1371/journal.pone.0038013.

Wu, J., Petralia, R. S., Kurushima, H., Patel, H., Jung, M-y., Volk, L., Chowdhury, S., Shepherd, J. D., Dehoff, M., Li, Y., Kuhl, D., Huganir, R. L., Price, D. L., Scannevin, R.,

Troncoso, J. C., Wong, P. C., Worley, P. F., 2011. Arc/Arg3.1 regulates an endosomal pathway essential for activity-dependent β-amyloid generation. Cell 147 (3), 615-628. doi: 10.1016/j.cell.2011.09.036.

Xu, Q., Bernardo, A., Walker, D., Kanegawa, T., Mahley, R W., Huang, Y., 2006. Profile and regulation of apolipoprotein E (ApoE) expression in the CNS in mice with targeting of green fluorescent protein gene to the ApoE locus. J. Neurosci. 26 (19), 4985-4994. doi: 10.1523/JNEUROSCI.5476-05.2006.

Zhou, L., Brouwers, N., Benilova, I., Vandersteen, A., Mercken, M., Van Laere, K., Van Damme, P., Demedts, D., Van Leuven, F., Sleegers, K., Broersen, K., Van Broeckhoven, C., Vandenberghe, R., De Strooper, B., 2011. Amyloid precursor protein mutation E682K at the alternative β-secretase cleavage β'-site increase Aβ generation. EMBO Mol. Med. **3 (5),** 291-302. doi: 10.1002/emmm.201100138.

## Figure Legends

**Figure 1. Aβ accumulation in the brain of APP-KI mice with or without human apoE throughout the aging process**

Brain Aβ levels of APP-KI (blue), APP-KI/apoE4-KI (red), and APP-KI/apoE3-KI (green) mice at 3, 5, 9, 13, and 21 months old were examined for Aβ40 (**A**) and Aβ42 (**B**). The amounts of Aβ42 are compared among three mouse models at the indicated ages (**C**). Statistical significance was determined by one-way ANOVA with Tukey's post hoc test for multiple comparisons (means ± S.E.; $n = 3–7$; $*p < 0.05$, $**p < 0.01$, $****p < 0.0001$).

**Figure 2. Aβ42 levels in the CSF and CVF of APP-KI mice with or without human apoE**

Aβ42 in cerebrospinal fluid (CSF) (**A-C**) and cerebroventricular fluid (CVF) (**D**) of APP-KI (blue), APP-KI/apoE4-KI (red), and APP-KI/apoE3-KI (green) mice at 3 (**A**), 7 (**B**), 14 (**C**), and 6–7 (**D**) months old were quantified by sELISA. Statistical significance was determined by one-way ANOVA with Tukey's post hoc test for multiple comparisons (means ± S.E.; $n = 3–5$; $*p < 0.05$, $**p < 0.01$, $****p < 0.0001$).

**Figure 3. Brain apoE levels in early- and late-aged APP-KI/apoE-KI mice**

Human apoE levels in the cerebral cortex and hippocampus in APP-KI (M), APP-KI/apoE4-KI (E4), and APP-KI/apoE3-KI (E3) mice at 13 and 21 months old were quantified by immunoblotting with anti-human apoE, anti-APP, and anti-α-tubulin antibodies (**A)**. Band density was standardized against the density of α-tubulin, and the value of apoE4 was assigned a reference value of 1.0 **(B)**. The levels were compared between 13- and 21-month-old apoE3 (green) and apoE4 (red) mice with unpaired Student's t-test (means ± S.E.; $n = 3$; $*p < 0.05$).

**Figure 4. Genes with altered expression in APP-KI/apoE3-KI and APP-KI/apoE4-KI mice during early and late aging**

Venn diagrams indicate the numbers of specifically identified genes and commonly identified genes for APP-KI/apoE3-KI and APP-KI/apoE4-KI mice versus APP-KI mice at 13 **(A)** and 21 **(B)** months of age. Detailed results of respective genes are shown in **Supplementary Table 1**.

**Figure 5. MA plot of genes with altered expression in the brain of APP-KI/apoE3-KI and APP-KI/apoE4-KI mice compared with APP-KI mice**

MA plots show the difference in gene expression in the cerebral cortex and hippocampus of APP-KI/apoE3-KI (upper graph) and APP-KI/apoE4-KI (lower graph) mice compared with APP-KI mice at 13 months old **(A)** and 21 months old **(B)**. The graphs include only

differentially regulated genes between APP-KI/apoE3-KI and APP-KI, and between APP-KI/apoE4-KI and APP-KI. The red dots indicate genes whose expression changed significantly in apoE4 mice, and the green dots indicate genes whose expression changed significantly in ApoE3 mice. The orange dots represent genes that share common alterations in expression in apoE3 and apoE4 mice. All genes that displayed significant changes in their expression are described in **Supplementary Table 1**.

**Figure 6. Quantification of gene expression by qPCR**

Selected data from qPCR analysis of 12 genes (Table 1). The expression profiles of four genes from among these 12 genes selected from RNA-seq coincided with the results from RT-qPCR. Statistical significance was determined by Student's t-test (means ± S.E.; $n = 4$ (two biological replicates with two technical replicates). $*p < 0.05$, $**p < 0.01$, $***p < 0.001$, n.s: not significant; 13M, 13-month-old; 21M, 21-month-old.

**Supplementary Figure Legends**

**Supplementary Figure S1. GO terms enriched in APP-KI/apoE4-KI and APP-KI/apoE3 mice**

Selected results from gene ontology analysis of brain transcriptome ranked by fold changes in gene expression in control vs. apoE3- or apoE4-KI mice. GO terms enriched in indicated conditions are shown (**A-F**). The value of axis indicates -log10 *p*-value. **(A)** Specific terms of APP-KI/apoE3 mice at 13 months of age. The top three clusters among significant terms (FDR<0.05) are shown. **(B)** Specific terms of APP-KI/apoE4 mice at 13 months of age. A top cluster (FDA<0.05) is shown. **(C)** Specific terms that are common in APP-KI/apoE3 and APP-KI/apoE4 mice at 13 months of age. The top three clusters among significant terms (FDR<0.05) are shown. **(D)** Specific terms of APP-KI/apoE3 mice at 21 months of age. The top four clusters among significant terms (FDR<0.05) are shown. **(E)** Specific terms of APP-KI/apoE4 mice at 21 months of age. The top two clusters among significant terms (FDR<0.05) are shown. **(F)** Specific terms that are common in APP-KI/apoE3 and APP-KI/apoE4 mice at 21 months of age. The top three clusters among significant terms (FDR<0.05) are shown.

**(A) Genes with altered expression in 13-month-old human apoE mice**

| | Gene name | 13-month-old | | Function and relationship with AD (related references) |
|---|---|---|---|---|
| | | apoE3 | apoE4 | |
| **1** | ***SgK1*** | ↓ | | Serum-/-glucocorticoid kinase 1(sSDG1), the upregulation promotes tau pathology. (*Human Mol. Genet.* 2021, 30, 1693) |
| **2** | ***Arc*** | ↓ | ↓ | Regulates the endosomal pathway of Ab generation. *Arc*-KO reduces Ab load. (*Cell* 2011, 147, 615-628) |
| **3** | ***Trem2*** | ↓ | ↓ | Type I membrane protein associates with TYRO, the complex activates microglia to increase phagocytosis and cytokine production. (*NEJM.* 2013, 368,117) |
| **4** | ***Atp5h*** | | ↓ | ATP synthase H+ transporting mitochondrial Fo. Important function in ATP generation. AD risk by GWAS. *(Mol. Psych.* 2013, 19, 682) |
| **5** | ***Ide*** | | ↓ | Insulin-degrading enzyme degrades Ab. (*Neurobiol. Aging* 2006, 27, 190) |
| **6** | ***Vgf*** | | ↑ | Vgf is the nerve growth factor inducible. Key regulator of AD. VGF increased in x5 FAD mice. (*Nat Commun.* 2020, 11, 3942 ) |

**(B) Genes with altered expression in 21-month-old human apoE mice**

| | Gene name | 21-month-old | | Function, relationship with AD (Related references) |
|---|---|---|---|---|
| | | apoE3 | apoE4 | |
| **7** | ***Ndrg2*** | | ↑ | α/β-hydrase fold protein. Upregulated in LAD. (*Neurobiol.* Dis. 2004, 16, 48). |
| **8** | ***Abca1*** | | ↑ | Cholesterol transporter, a risk of LAD. Lack of Abca1 decreases apoE. (*Neurobiol. Aging* 2007, 28, 856). |
| **9** | ***Timp3*** | | ↑ | Metalloprotease inhibitor. The level increases in AD. (*J. Neurosci.* 2007, 27, 10895) |
| **10** | ***Apod*** | | ↑ | Related to ROS-induced glial lipid droplet. (*PNAS* 2021, 118, e2112095118) |
| **11** | ***Calr*** | ↑ | | Calreticulin, ER protein, regulates gene expression mediated by nuclear hormone receptor. (*Int. J. Mol. Sci.,* 2014, 15, 21740) |
| **12** | ***Vegfa*** | ↑ | | Gene variant is protective against AD. (*Aging* 2022, 14, 2524) |
| **(6)** | ***Vgf*** | ↑ | | Described above (A) |
| **(3)** | ***Trem2*** | ↓ | | Described above (A) |

**Table 1. Genes whose expression changed in an apoE isotype-specific or age-dependent manner, and their reported possible roles in the brain pathophysiology of AD.**

The expression of 12 genes was significantly changed in a human apoE isotype-specific or age-dependent manner in early- (**A** 13-month-old) and late-aged (**B** 21-month-old) apoE4 and apoE3 mice, as assessed by RNA-seq analysis. The arrows indicate gene upregulation (red) and downregulation (blue). Possible roles in the brain Aβ load and/or AD pathology are shown in the right-most column.

**Titles of Supplementary Tables and Data**

**Supplementary Table 1.** List of genes whose expression was significantly changed in APP-KI/apoE3-KI and APP-KI/apoE4-KI mice versus APP-KI mice at 13 and 21 months of age.

**Supplementary Table 2.** Primer sequence used in RT-qPCR analysis

**Supplementary Data (Text Files) Gene expression analysis of 13- and 21-month-old mice**
The following two txt files are not included in single PDF files for review because the file occupied >2000 pages when the files were transformed into PDF files. The editor and reviewers can access the following site to obtain two txt files.
https://www.dropbox.com/scl/fo/76jwscahy76qjzjcn083f/h?dl=0&rlkey=1rxnqh1akwkg114n0djtdyzsm
**DESeq2_result_13M_ALL_gene.info.txt**
**DESeq2_result_21M_ALL_gene.info.txt**

**Supplementary Data (Excel File)** Gene ontology analysis.
The excel file (Supplementary Data_GO.xlsx) was transformed into the following 6 PDF files and attached to the main text file to make a single PDF file for review.
**Supplementary Data_GO_13month_E3.pdf (Data of Supplementary Figure S1A)**
**Supplementary Data_GO_13month_E4.pdf (Data of Supplementary Figure S1B)**
**Supplementary Data_GO_13month_common.pdf (Data of Supplementary Figure S1C)**
**Supplementary Data_GO_21month_E3.pdf (Data of Supplementary Figure S1D)**
**Supplementary Data_GO_21month_E4.pdf (Data of Supplementary Figure S1E)**
**Supplementary Data_GO_21month_common.pdf (Data of Supplementary Figure S1F)**

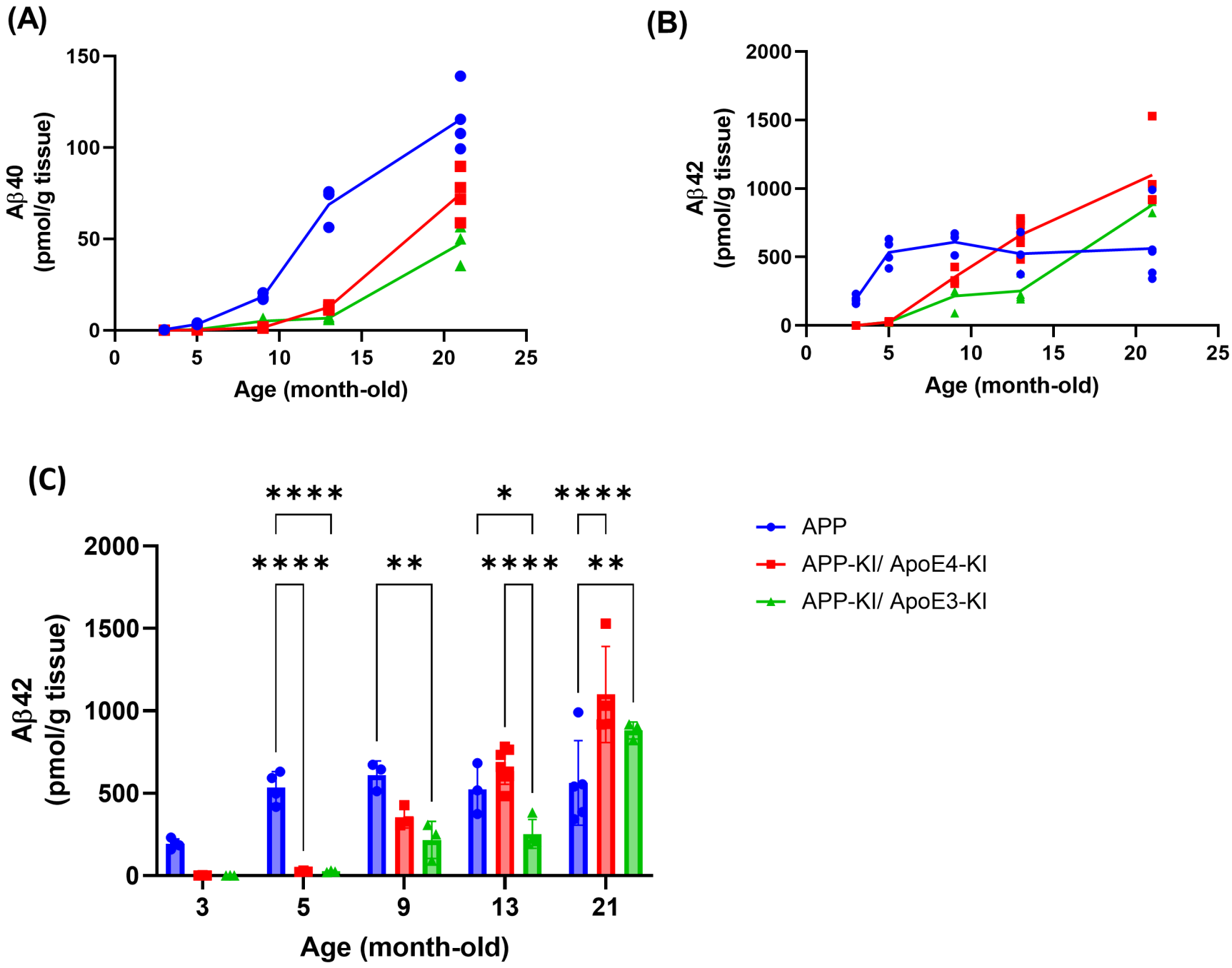
(A)
Aβ40 (pmol/g tissue)
150
100
50
0
0
5
10
15
20
25
Age (month-old)
(B)
Aβ42 (pmol/g tissue)
2000
1500
1000
500
0
0
5
10
15
20
25
Age (month-old)
(C)
Aβ42 (pmol/g tissue)
2000
1500
1000
500
0
****
****
**
*
****
****
**
3
5
9
13
21
Age (month-old)
APP
APP-KI/ ApoE4-KI
APP-KI/ ApoE3-KI

Fig.1

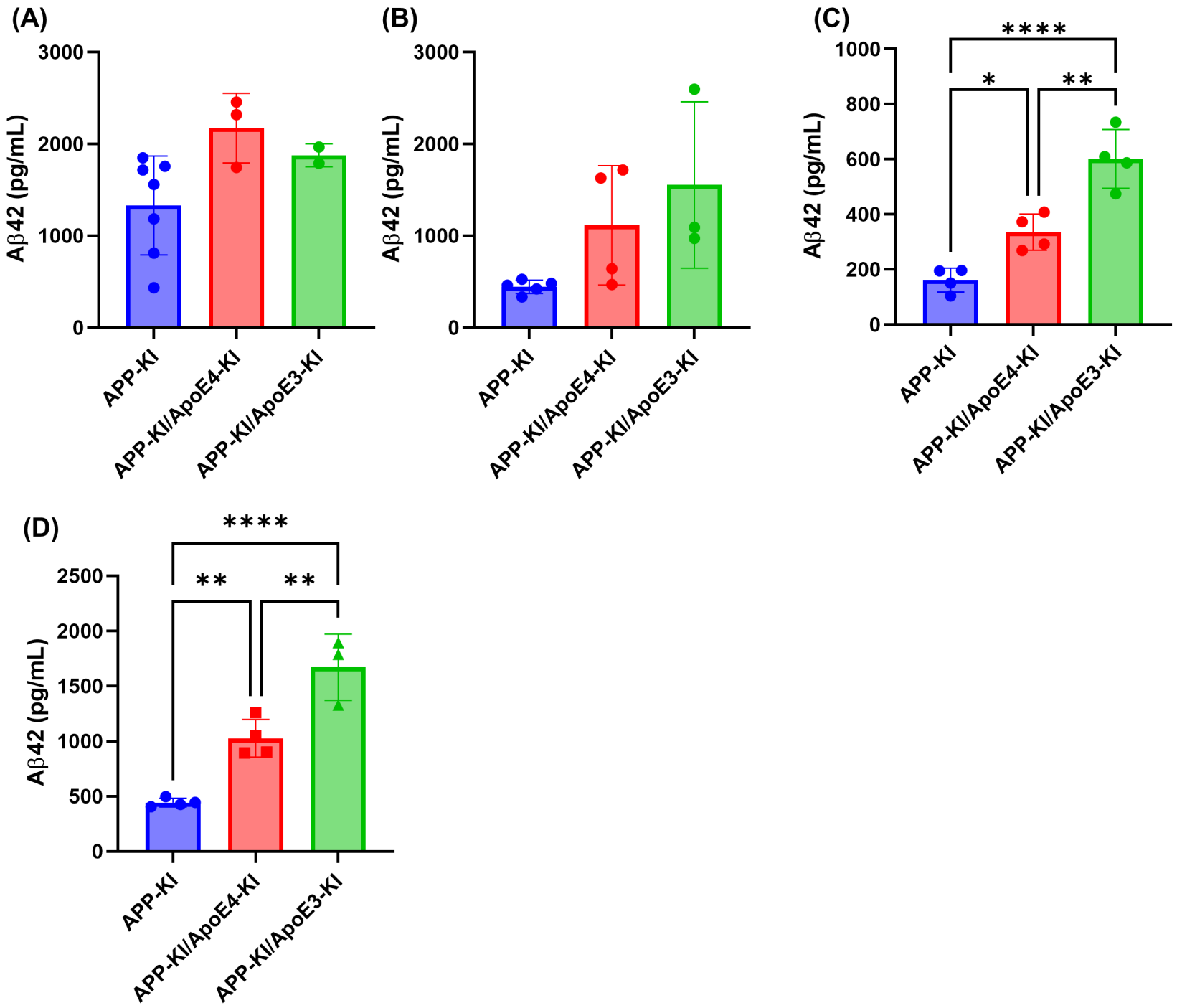
(A)
Aβ42 (pg/mL)
3000
2000
1000
0
APP-KI
APP-KI/ApoE4-KI
APP-KI/ApoE3-KI
(B)
Aβ42 (pg/mL)
3000
2000
1000
0
APP-KI
APP-KI/ApoE4-KI
APP-KI/ApoE3-KI
(C)
Aβ42 (pg/mL)
1000
800
600
400
200
0
****
*
**
APP-KI
APP-KI/ApoE4-KI
APP-KI/ApoE3-KI
(D)
Aβ42 (pg/mL)
2500
2000
1500
1000
500
0
****
**
**
APP-KI
APP-KI/ApoE4-KI
APP-KI/ApoE3-KI

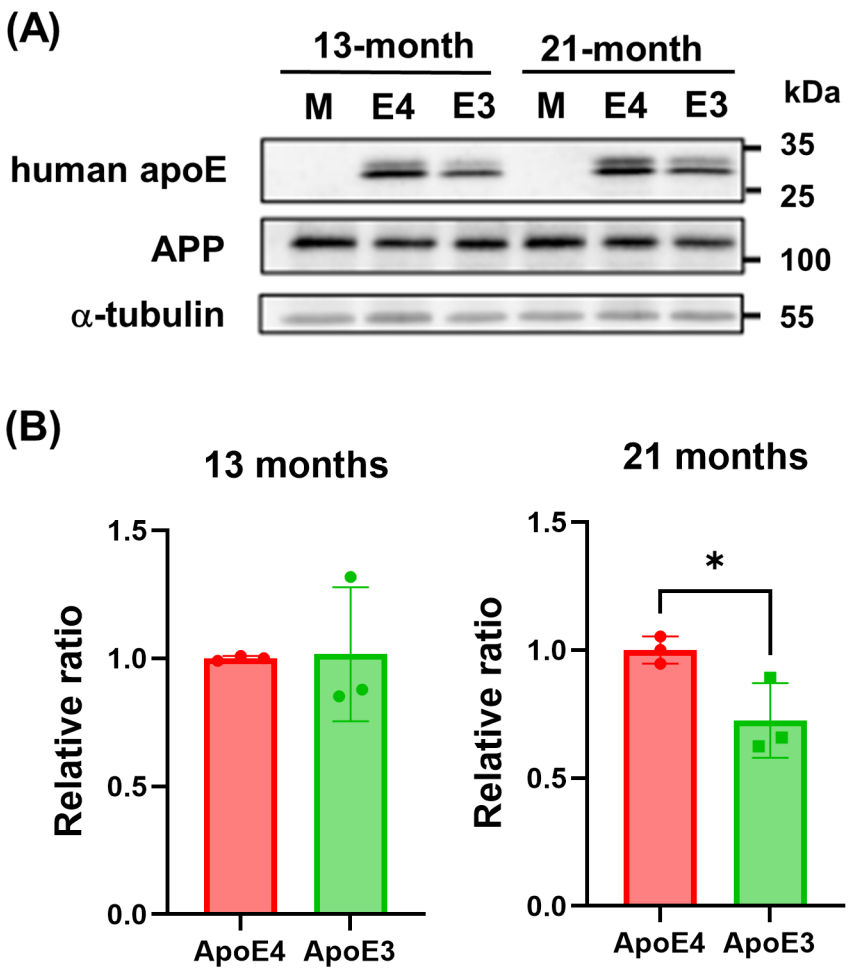
(A)
13-month
21-month
M
E4
E3
M
E4
E3
kDa
human apoE
35
25
APP
100
α-tubulin
55
(B)
13 months
21 months
Relative ratio
1.5
1.0
0.5
0.0
ApoE4
ApoE3
*

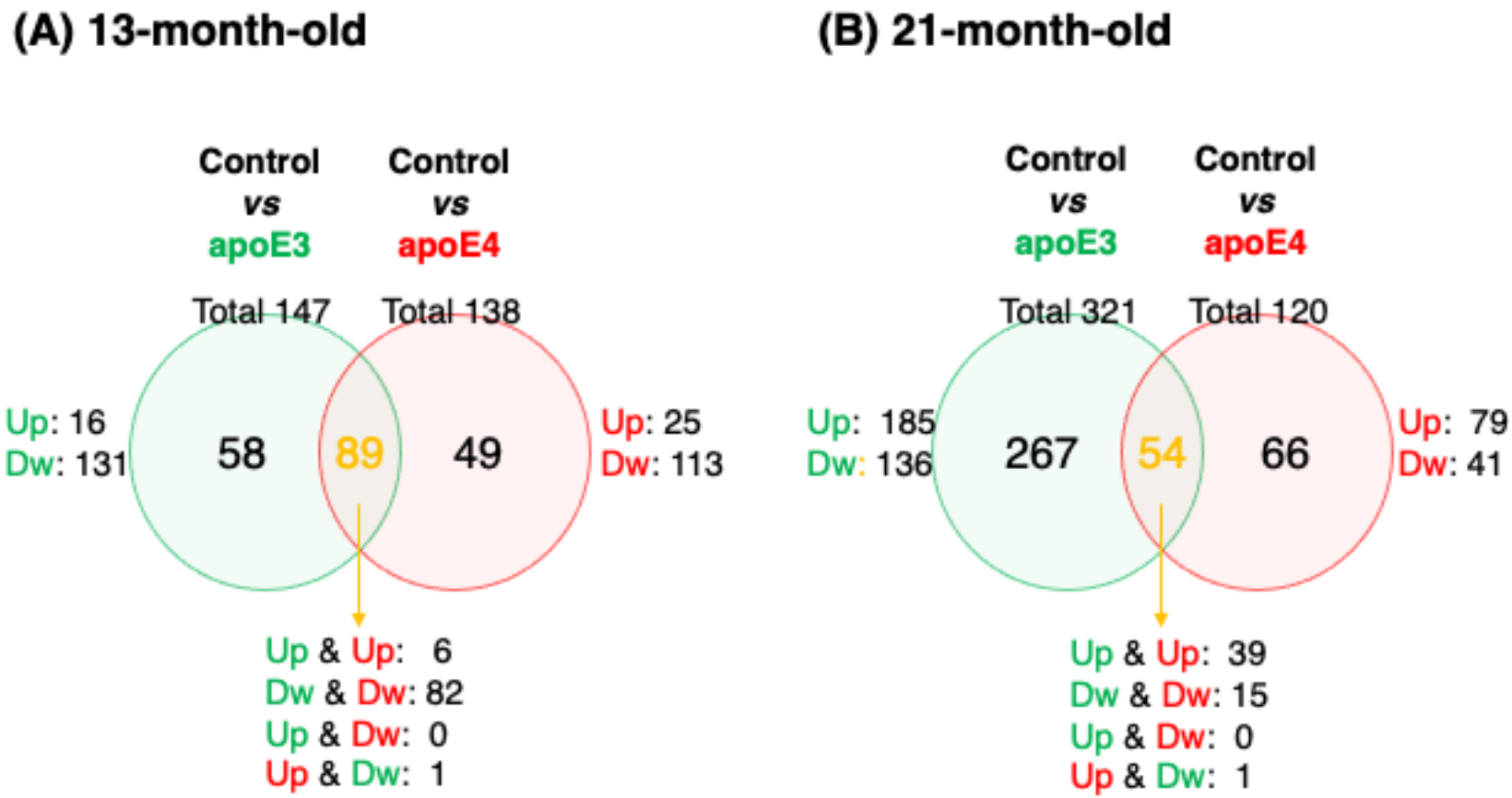
(A) 13-month-old
Control vs apoE3
Control vs apoE4
Total 147
Total 138
Up: 16
Dw: 131
58
89
49
Up: 25
Dw: 113
Up & Up: 6
Dw & Dw: 82
Up & Dw: 0
Up & Dw: 1
(B) 21-month-old
Control vs apoE3
Control vs apoE4
Total 321
Total 120
Up: 185
Dw: 136
267
54
66
Up: 79
Dw: 41
Up & Up: 39
Dw & Dw: 15
Up & Dw: 0
Up & Dw: 1

Fig. 4

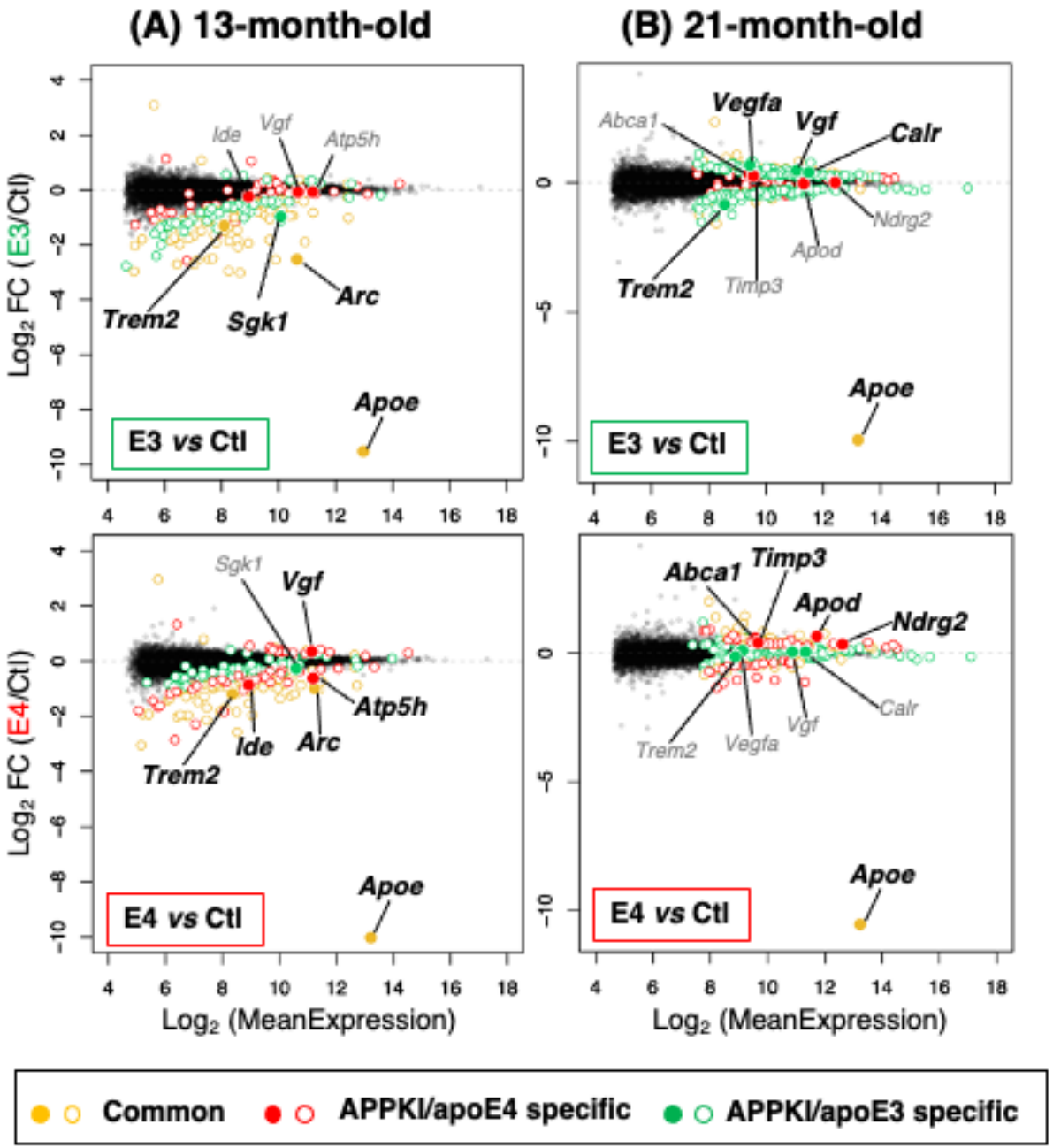
(A) 13-month-old
(B) 21-month-old
Log2 FC (E3/Ctl)
Log2 FC (E4/Ctl)
Log2 (MeanExpression)
E3 vs Ctl
E4 vs Ctl
Ide
Vgf
Atp5h
Trem2
Sgk1
Arc
Apoe
Abca1
Vegfa
Calr
Ndrg2
Apod
Timp3
Common
APPKI/apoE4 specific
APPKI/apoE3 specific

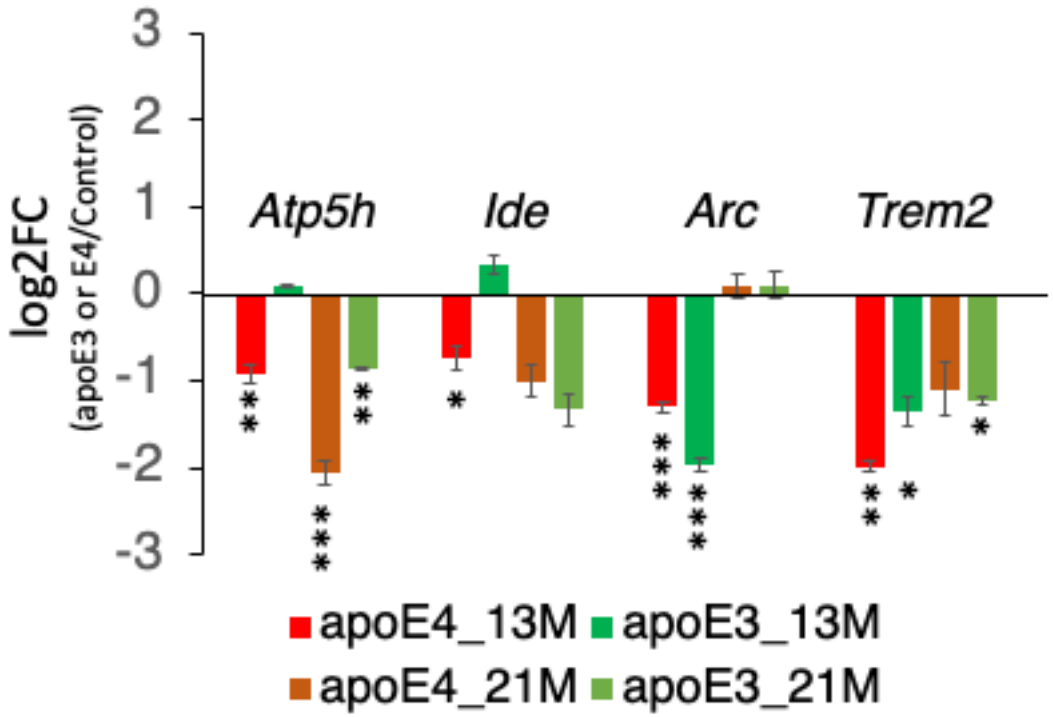
log2FC
(apoE3 or E4/Control)
3
2
1
0
-1
-2
-3
Atp5h
Ide
Arc
Trem2
apoE4_13M
apoE3_13M
apoE4_21M
apoE3_21M

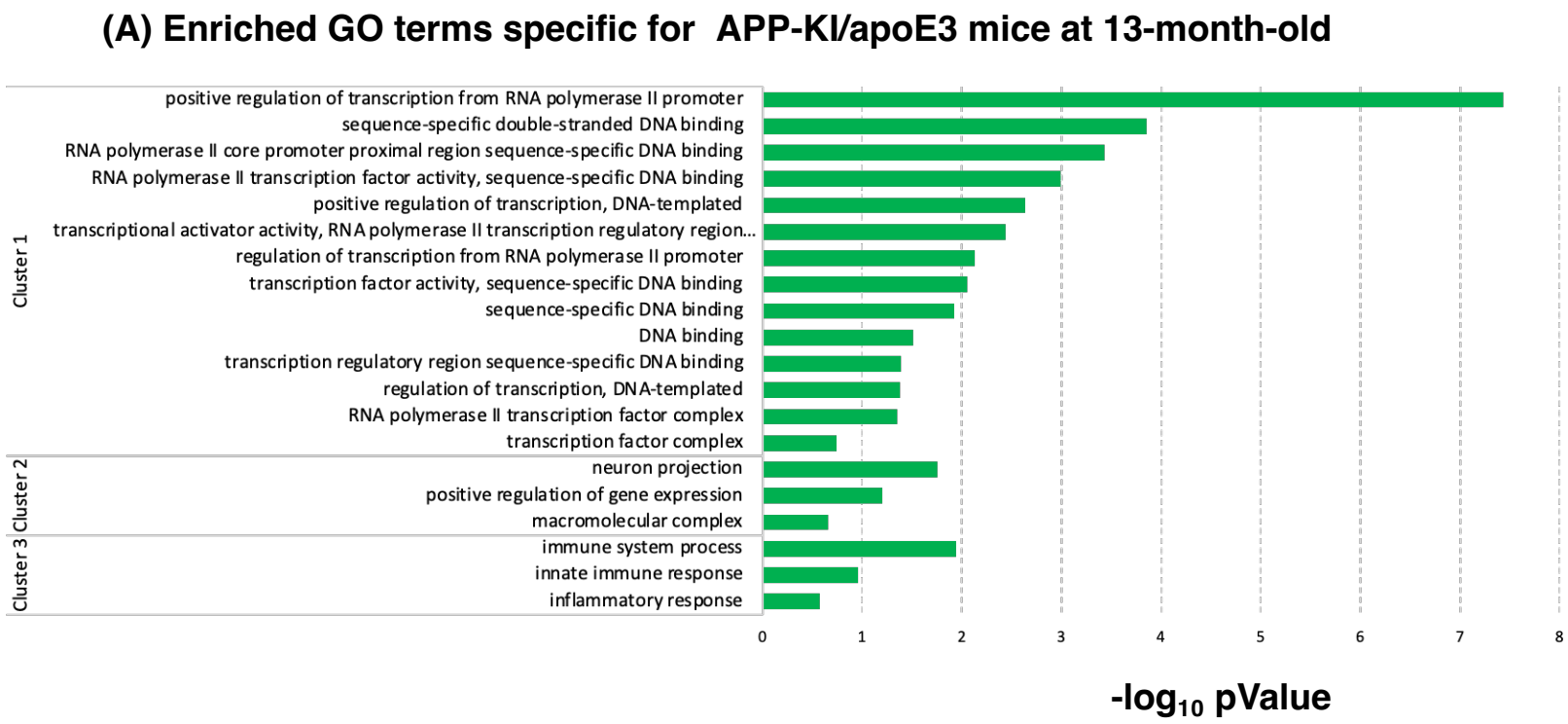


**Supplementary Figure S1A**

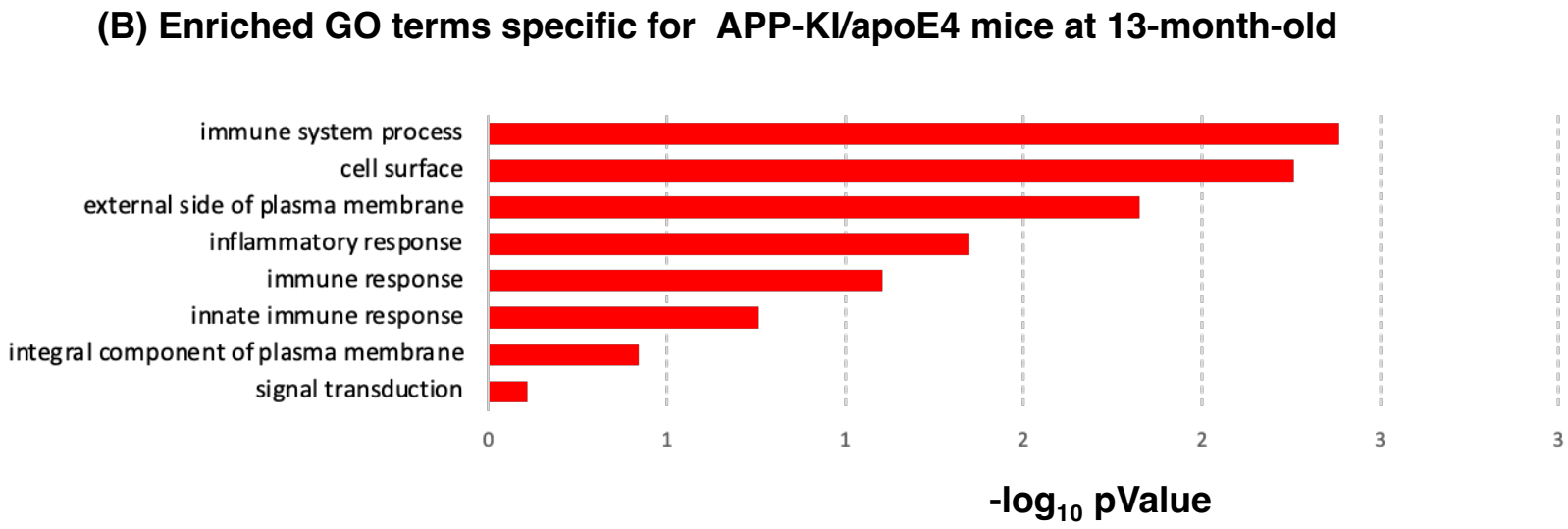


**Supplementary Figure S1B**

## (C) Enriched GO terms common for APP-KO/apoE3 and APP-KI/apoE4 mice at 13-month-old

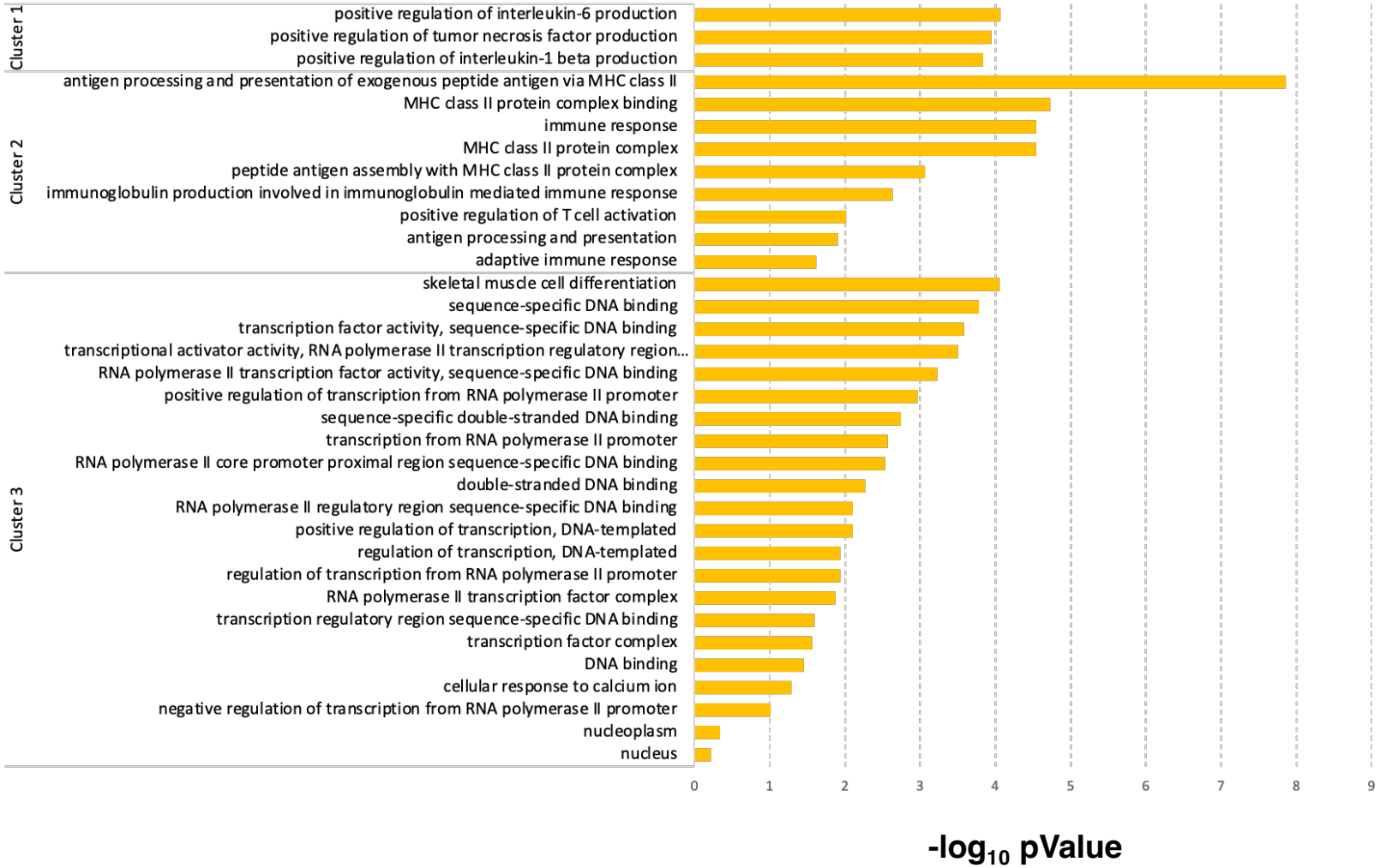


**Supplementary Figure S1C**

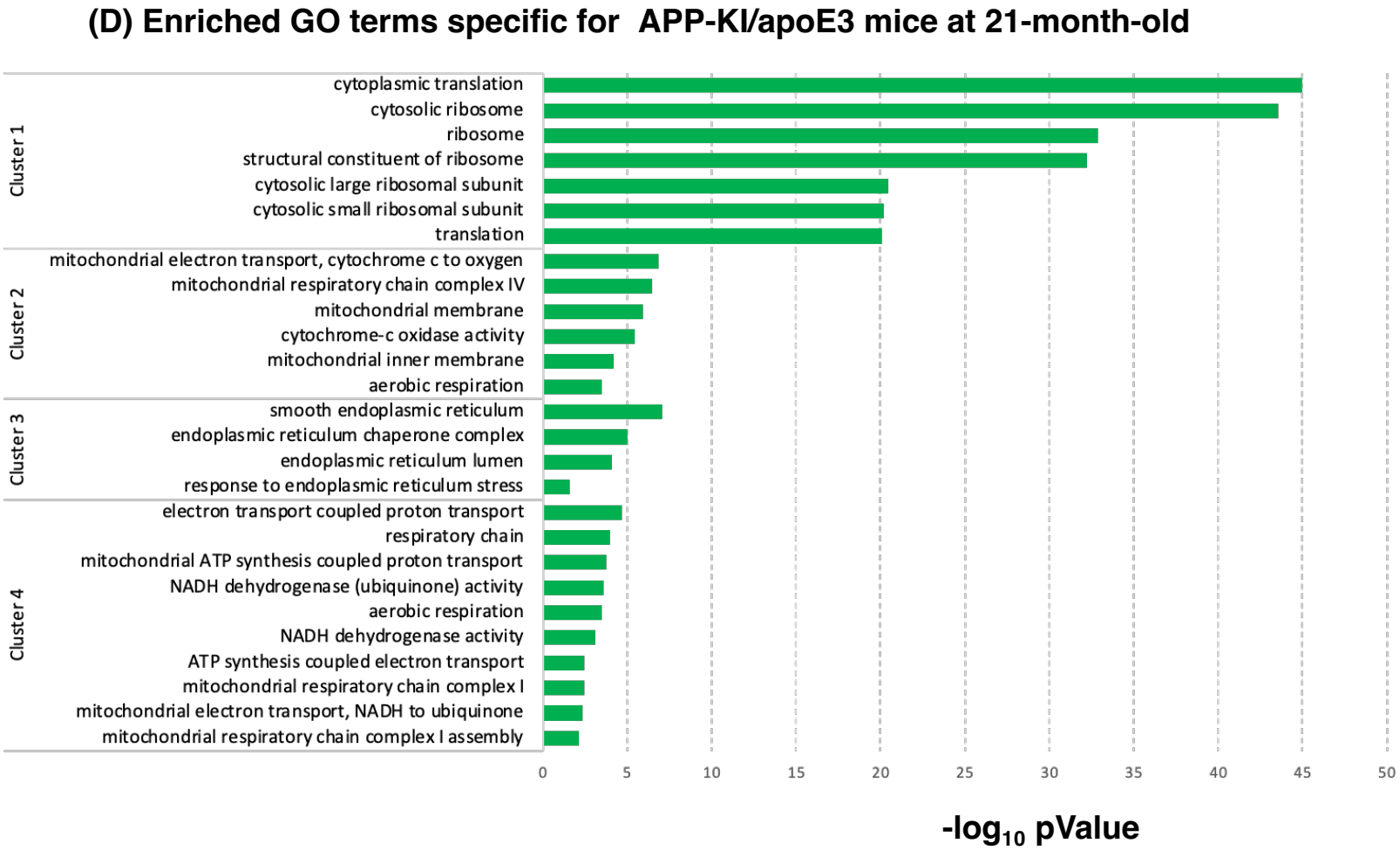


**Supplementary Figure S1D**

**(E) Enriched GO terms specific for APP-KI/apoE4 mice at 21-month-old**

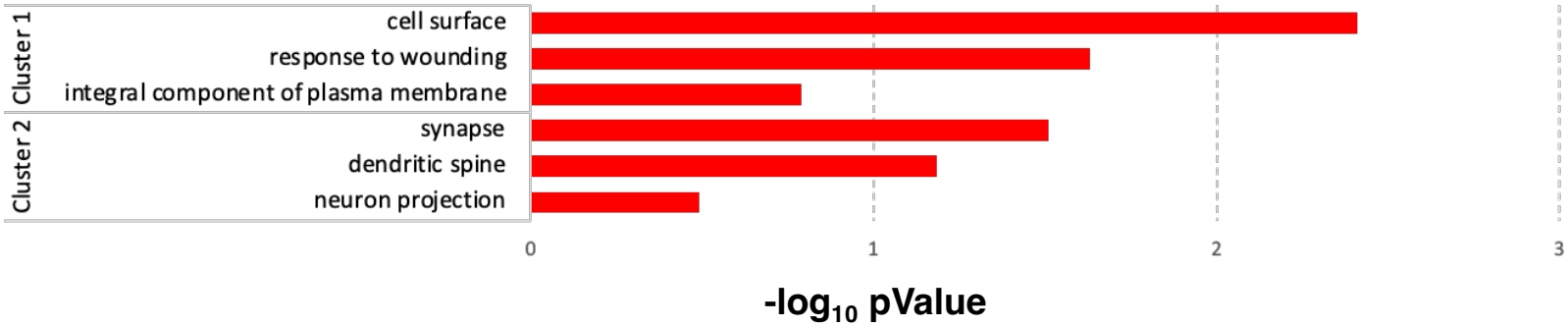


**Supplementary Figure S1E**

**(F) Enriched GO terms common for APP-KO/apoE3 and APP-KI/apoE4 mice at 21-month-old**

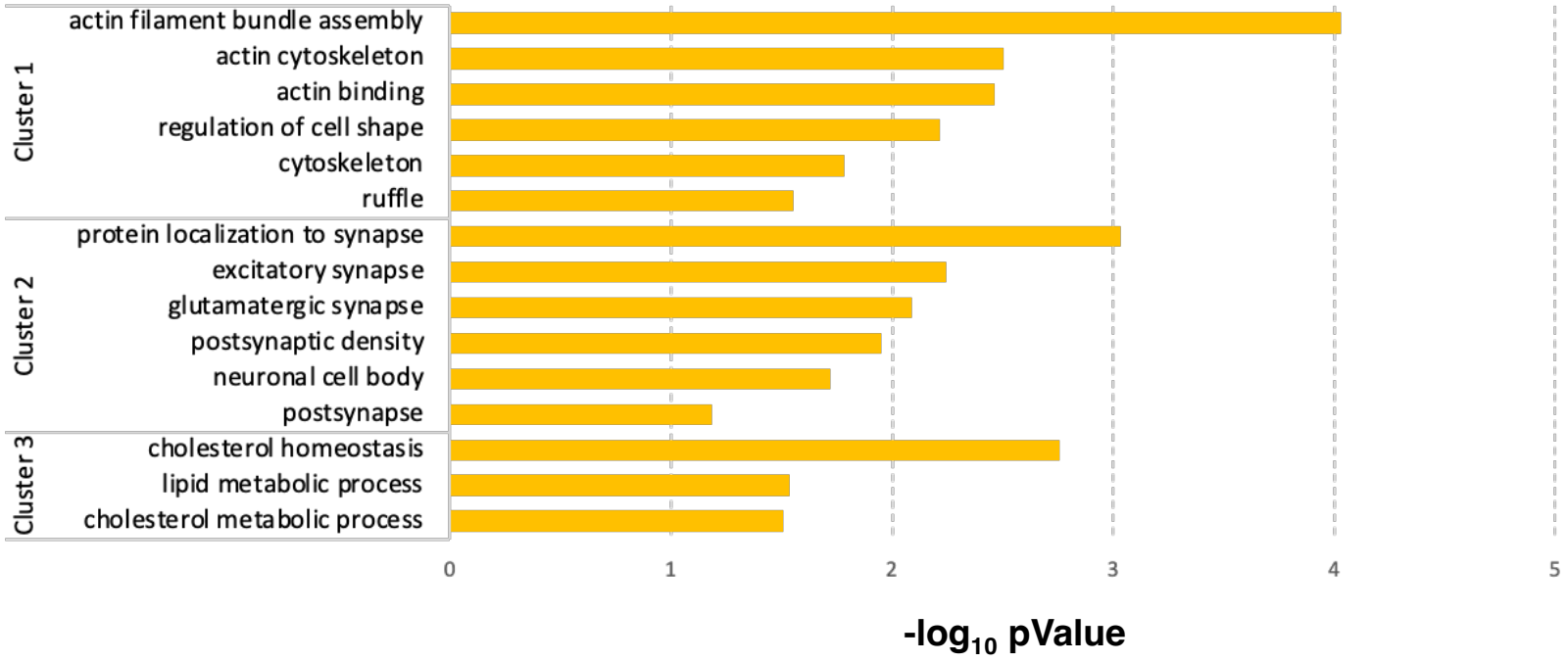


**Supplementary Figure S1F**

## 13 months old

| 13M ApoE4 (specific) | gene names |
|---|---|
| Down | Eps8l1, Csf1, Kctd2, Ctsa, Nt5c, Slc11a1, Cst3, Tlr2, Bhlhe40, A2m, Ryr1, Slc37a2, Tspoap1, Atp5h, Hid1, H2-Aa, Btaf1, Npas4, Phldb1, Cdr2l, Siglech, Wdfy4, Cx3cr1, Rab7b, Capg, Ide, Fcer1g, H2-K1, Trank1, Lyz2, Neat1 |
| Up | Etnppl, Dynll2, Xbp1, Paqr8, Hspa5, Spred1, Elavl4, Slc17a6, Galnt9, Lars2, Pcdh17, Kirrel2, Vgf, Scg2, Gfod1, Sae1, B3galt5, CT010467.1 |

| 13M ApoE3 (specific) | gene names |
|---|---|
| Down | Axl, Dio2, Hspa8, Dusp6, Sgk1, Igf1, Ddit4, Per1, Nfkbia, Gng4, Map3k1, Clu, Slc38a2, Sall3, Doc2g, Cd63, Mfap3l, Eomes, Trib1, Csrnp1, Ablim3, Egr3, Inpp5j, Tiparp, Dusp5, Arl4d, Adrb1, Midn, Pim3, Dnajb5, Klf10, Aspg, Cd84, Gpr34, Dlx1, Atf4, Lgr6, Tlr7, Tob2, Cd14, Irf2bp2, Klf2, Cebpd, Omp, Nlrc5, Mafb, Sox4, 1700016P03Rik |
| Up | Nalcn, Efnb3, Ptgds, 6330403K07Rik, Ache, Syt2, Ndst4, Vamp1, Minar2, Caln1 |

| 13M ApoE4 & E3 (common) | gene names |
|---|---|
| Down | Apoe, Fosb, Man2b1, Ctsd, Gadd45b, Lpl, Fcrls, Ctsz, Cyth4, Cd68, Ccl6, Fabp7, Plek, Btg2, Gfap, Serpina3n, Fos, Ly86, Ctsl, Cd180, Hexb, Plau, Ctsb, Arc, Itgb5, Adamts1, Nr4a1, Trem2, Sik1, Dusp1, Cd74, Csf1r, Hexa, Gusb, Igfbp5, Ptprc, Ncf2, Atf3, Fcgr2b, Nr4a2, Ccn1, Nr4a3, Laptm5, Csf3r, Fosl2, Gpnmb, Lag3, Cd9, Tyrobp, Itgax, Dcx, Mamdc2, Lgals3bp, Grn, Nudt19, C1qa, C1qc, C1qb, Ppp1r14a, Egr1, Ctss, Hipk4, Erf, Irf8, Tent5c, Mpeg1, Junb, Ier2, Fcgr3, H2-Eb1, B2m, Gm8995, Zfp772, Cst7, Egr4, C4b, H2-Ab1, Clec7a, Apold1, AU020206, 9330104G04Rik |
| Up | Pnmal1, Zfp14, Vsnl1, Arhgap35, Unc13c, Gm45104 |

## 21 months old

| 21M ApoE4 (specific) | gene names |
|---|---|
| Down | Tomm40, Kctd2, Mrpl58, Nt5c, Aspa, Erbin, Aqp4, Fgfr2, Ugt8a, Sox10, Atp5h, Hid1, Rps29, Mboat7, Rps21, Gpr37, Cdr2l, Tmem88b, Gm13340, Gm29216 |
| Up | Ranbp2, Ndrg2, Slc1a2, Slc1a3, Rdh13, Slc41a1, Abca1, Sdc4, Arid5b, Timp3, Ankrd33b, Apod, Epas1, Camk2a, Prdx6, Mal, F3, Bhlhe40, Mt1, Mobp, Chst2, Ucp2, Lgals3bp, Arl4d, Lars2, Mtcl1, Ly6a, Gm23935, CT010467.1 |

| 21M ApoE3 (specific) | gene names |
|---|---|
| Down | Rpl13, Tmem242, Pvalb, Tmbim1, Rps9, Ctsd, Rplp1, Rps18, Sdhb, Rps25, Rps5, Cox6c, Lpl, H3f3b, Rpl19, Cox7c, Plek, Rps27a, Hif1a, Npc2, Fdft1, Ly86, Ctsl, Hexb, Elovl7, Stmn4, Sqle, Litaf, Sod1, Scg5, Trem2, Cox7a2l, Rps14, Cd74, Fth1, Rps26, Echs1, Rplp2, Rpl14, Dbi, Fabp5, Rps3a1, Rps20, Laptm5, Prdx1, Sorcs2, Spp1, Actb, Gpnmb, Cd9, Tyrobp, Rps3, Itgax, Msmo1, Cox4i1, Cox7a2, Tgfbr2, Rpsa, Gucy1a1, Ndufa13, C1qa, C1qc, C1qb, Ppp1r14a, Fau, Ctss, Atp5j2, Rpl12, Rpl21, Selenow, Rpl37, Nrep, Rps2, Cirbp, Mpeg1, Rab2a, Rpl9, Rps8, Rpl29, Nrsn1, Rps23, Tmsb4x, Cx3cr1, Mllt11, Ech1, Atpif1, Rpl36, Rpl5, Dbp, Rpl3, Gm10076, Rpl35a, B2m, Cox5b, Rps17, Rpl34, Rpl17, Actg1, Rps15, mt-Nd1, mt-Co1, mt-Nd4, mt-Nd5, mt-Nd6, mt-Cytb, Rplp0, Cst7, Lyz2, Chchd2, H2-D1, Rpl31, Gpx4, AI593442, Rpl39, Rps13, Inafm1, Neat1, Rpl41, Hmgcs1, H1f0 |
| Up | Mef2d, Chordc1, Kmt2a, Calr, Cacna1e, Cbfa2t3, Usp19, Dio2, Hnrnph1, Hipk1, Bcr, Etv5, Klhl3, Actn1, Hivep2, Hspa8, Tnr, Dync1h1, P4ha1, Hsp90b1, Ccar1, Eif4ebp2, Pdia6, Rock2, Klhl29, Pxdn, Helz, Mink1, Luc7l3, Foxg1, Rab15, Trim9, Pfkp, Unc79, Ryr2, Iqgap2, Bmp1, Pdzd2, Trio, Slc38a2, Plec, Abcc5, Son, Paxbp1, Scn8a, Cdkn1a, Synj2, Vegfa, Brd4, Srsf7, Spire1, Nedd4l, Pdia4, Fn1, Ccnt2, Ahctf1, Plxna2, Hspa5, Spred1, Snph, Rbm39, Srsf10, Sfpq, Ptpru, Pitpnm2, Ncor2, Hsph1, Tra2a, Smg1, Atp11a, Mcf2l, Cx3cl1, Mast3, Hyou1, Smad3, Nktr, Manf, Atxn2l, Ank2, Pkd1, Galnt9, Rbfox2, Arhgap39, Gria2, Igsf9b, Cbl, Cmip, Adgrb1, Ythdc1, Lrrk2, Anln, Srrt, Dmxl1, Vgf, Shank2, Lzts3, Ppp1r16b, Wnk2, Pde4dip, Mical2, Shank1, Zmynd8, Hip1, Gramd1b, Lrp1, Daam2, Inhba, Slc24a4, Sgsm1, Safb2, Sipa1l1, Smg7, Synpo, Ptpn11, Trrap, Basp1, Kmt2d, Acap2, Pdp1, Sorl1, Fam171a1, Kcnb1, Cacna1c, Pcdh1, Mical3, Kcnf1, Gpr17, Map1b, Shisa7, Shisa6, Fmnl1, Ryr3, Sptan1, Sez6l, Arhgap35, Csmd1, Dlgap4, Trank1, Sptbn2, Ank3, Safb, Cdr1os, Fat3, Syne1, A330023F24Rik, Mir124a-1hg |

| 21M ApoE4 & E3 (common) | gene names |
|---|---|
| Down | Rnd2, Apoe, Ptgds, Septin4, Nr1d1, Rps24, Car2, Ldlr, Nudt19, Scd1, Insig1, Opalin, Rpl38, S100a16, Gm42372 |
| Up | Vwf, Plin4, Htra1, Homer1, Mertk, Etnppl, Fam107a, Myh9, Fkbp5, Baiap2, Nptx1, Paqr8, Clk1, Glul, Slc2a1, Ago3, Add2, Adipor2, Tsc22d3, Gpt2, Bsn, Klf9, Dnajb5, Ttyh3, Herc1, Slc7a5, Gjb6, Enc1, Sbk1, Spred2, Islr2, Gfod1, Klf13, Ezr, Per2, Zbtb16, Ahnak, Wipf3, Lrrc10b |

## apoE4 mice

| both 13M and 21M ApoE4 | gene names |
|---|---|
| Down | Apoe, Eps8l1, Kctd2, Nt5c, Atp5h, Hid1, Nudt19, Cdr2l, Zfp772, 9330104G04Rik, Gm42372 |
| Up | Homer1, Etnppl, Paqr8, Lars2, Kirrel2, Gfod1, CT010467.1, Gm45104 |

## apoE3 mice

| both 13M and 21M ApoE3 | gene names |
|---|---|
| Down | Apoe, Ctsd, Lpl, Plek, Ly86, Ctsl, Hexb, Trem2, Cd74, Laptm5, Gpnmb, Cd9, Tyrobp, Itgax, Nudt19, C1qa, C1qc, C1qb, Ppp1r14a, Ctss, Mpeg1, B2m, Cst7, Gm42372 |
| Up | Arhgap35 |

Supplementary Table 1

| | gene | forward | reverse |
|---|---|---|---|
| 1 | *Sgk1* | TGGCACGCCTGAGTATCTGG | GCAGGCCGTAGAGCATCTCA |
| 2 | *Arc* | AAGCGGGACCTGTACCAGAC | CGTCCTGCACTTCCATACCC |
| 3 | *Trem2* | TCCCAAGCCCTCAACACCAC | GCTCCCATTCCGCTTCTTCAGG |
| 4 | *Atp5h* | GGCTGGGCGTAAACTTGCTC | CACATTGGCCCTGTAGTAAGCCC |
| 5 | *Ide* | GGCCATAGAGGACATGACAGAGG | CTTTATGTCTCCTCGGTGCGTC |
| 6 | *Vgf* | GTCCACCAAACTCCACCTGC | GAGCACTTCGTTCCAGTCCG |
| 7 | *Ndrg2* | CATCCAACACGCACCCAACC | CTTGGTCTCCAACCACCAGC |
| 8 | *Abca1* | TCAGCATCCTCTCCCAGAGC | GAGAACGGCCACATCCACAAC |
| 9 | *Timp3* | CATCGTGATCCGGGCCAAAG | CATCGTGATCCGGGCCAAAG |
| 10 | *Apod* | GAGCAACGTCTCAGAGCCAG | GCAGGAGTACACGAGGGCAT |
| 11 | *Calr* | CGTGAAGCTGTTTCCGAGTGG | CTCATAGGTGTTGTCTGGCCG |
| 12 | *Vegfa* | ACCCACGACAGAAGGAGAGC | GCACACAGGACGGCTTGAAG |
| control | *bact* | GCTGTGCTGTCCCTGTATGCCTCT | CTCAGCTGTGGTGGTGAAGC |

**Supplementary Table 2. Primer sequence used in RT-qPCR analysis**